Article:
Rubaiy, HN orcid.org/0000-0002-1489-5576, Seitz, T, Hahn, S et al. (8 more authors) (2018) Identification of an (−)-englerin A analogue, which antagonizes (−)-englerin A at TRPC1/4/5 channels. British Journal of Pharmacology, 175 (5). pp. 830-839. ISSN 0007-1188

https://doi.org/10.1111/bph.14128

Identification of an (-)-Englerin A analogue which antagonizes (-)-Englerin A at TRPC1/4/5 channels

Hussein N Rubaiy[1], Tobias Seitz[2], Sven Hahn[2], Axel Choidas[3], Peter Habenberger[3], Bert Klebl[3], Klaus Dinkel[3], Peter Nussbaumer[3], Herbert Waldmann[4], Mathias Christmann[2*], David J Beech[1*]

[1]School of Medicine, University of Leeds, Leeds, LS2 9JT, UK. [2]Institute of Chemistry and Biochemistry, Freie Universität Berlin, Takustraße 3, 14195 Berlin, Germany. [3]Lead Discovery Center GmbH, Otto-Hahn-Str. 15, D-44227 Dortmund, Germany. [4]Max- Planck-Institut für Molekulare Physiologie, Otto-Hahn-Straße 11, 44227 Dortmund, Germany.

*Authors for correspondence: Professor Mathias Christmann, Institute of Chemistry and Biochemistry, Freie Universität Berlin, Takustraße 3, 14195 Berlin, Germany. Telephone +49 (0) 30 83860182. Email mathias.christmann@fu-berlin.de. Professor David J Beech, Leeds Institute of Cardiovascular and Metabolic Medicine, School of Medicine, LIGHT Building, Clarendon Way, University of Leeds, Leeds LS2 9JT, UK. Telephone +44 (0) 113 343 4323. Email d.j.beech@leeds.ac.uk

BACKGROUND AND PURPOSE
(-)-Englerin A (EA) is a potent cytotoxic agent against renal cell carcinoma cells. It achieves its effects by activation of TRPC4/TRPC1 heteromeric channels. It is also an agonist at channels formed by the related protein, TRPC5. Here we sought an EA analogue which might enable better understanding of these EA effects.

EXPERIMENTAL APPROACH
Renal cell carcinoma A498 cells and HEK 293 cells overexpressing TRPC4 or TRPC5 were studied by intracellular Ca^{2+} measurement or whole-cell patch-clamp. The EA analogue A54 was generated by total synthesis.

KEY RESULTS
A54 had weak or no agonist activity at endogenous TRPC4/TRPC1 channels in A498 cells or TRPC4 or TRPC5 homomeric channels overexpressed in HEK 293 cells. A54 strongly inhibited EA-mediated activation of TRPC4/TRPC1 or TRPC5 and weakly inhibited activation of TRPC4. Studies of TRPC5 showed that A54 right-shifted the EA concentration-response curve without changing its slope, consistent with competitive antagonism. In contrast, TRPC5 activated by Gd^{3+} and TRPC4 activated by sphingosine-1-phosphate were not inhibited but potentiated by A54. A54 did not activate TRPC3 channels or affect activation of these channels by the agonist 1-oleoyl-2-acetylglycerol.

CONCLUSIONS AND IMPLICATIONS
The data suggest identification of a tool compound which could be useful for characterizing endogenous TRPC1/4/5 channels and understanding EA binding sites and their physiological relevance.

Abbreviations

TRPC, Transient Receptor Potential Canonical; EA, (-)-Englerin A; A54, Analogue 54; HEK 293 cells; human embryonic kidney 293 cells; A498 cells, human renal cell carcinoma cell line 498; Gd^{3+}, gadolinium ion.

Introduction

(-)-Englerin A is a natural product from Phyllanthus engleri, a South East African plant (Wu et al., 2017). It was found to have potent cytotoxic effects against some types of cancer cell cultured from kidney, breast, bone, brain, lung, hematopoietic, prostate and other cancers (Akbulut et al., 2015, Caropreso et al., 2016, Carson et al., 2015, Ratnayake et al., 2009, Sourbier et al., 2013). Subsequent studies reported in vivo efficacy against xenograft tumours generated in mice using 786-O and PC3 cancer cell lines, suggesting potential for a novel therapeutic strategy (Sourbier et al., 2013). Chemistry studies led to the development of efficient synthesis routes for (-)-Englerin A and derivatives of it and gave initial insights into structure-activity relationships (Radtke et al., 2011, Willot et al., 2009, Wu et al., 2017).

The Transient Receptor Potential Canonical (TRPC) proteins are a subfamily of the TRP super family and assemble as homo- and hetero-tetramers to form Ca^{2+}-permeable non-selective cationic channels (Abramowitz and Birnbaumer, 2009, Beech, 2013, Damann et al., 2008, Gaunt et al., 2016, Moran et al., 2011, Rubaiy, 2017). They appear to function in two clusters, TRPC1/TRPC4/TRPC5 (TRPC1/4/5) and TRPC3/TRPC6/TRPC7, which are distinguishable pharmacologically (Akbulut et al., 2015, Bon and Beech, 2013, Maier et al., 2015, Miller et al., 2011, Rubaiy et al., 2017b, Washburn et al., 2013, Rubaiy et al., 2017a).

TRPC1/4/5 channels are potently and strongly activated by EA whereas TRPC3 and TRPC6 channels are unaffected (Akbulut et al., 2015, Carson et al., 2015, Ludlow et al., 2017, Rubaiy et al., 2017b). EA-evoked cytotoxicity is TRPC4 dependent in A498 renal cell carcinoma and other cancer cell lines (Carson et al., 2015, Ludlow et al., 2017). TRPC5 is poorly expressed in many cancer cell lines but may be relevant in some cancer cell types (Carson et al., 2015, Ma et al., 2012). The role of TRPC1 is not completely understood but its involvement in the A498 cell and Hs578T triple-negative breast cancer cell death evoked by EA and relevance to the control of Na^+ versus Ca^{2+} permeability in these cells has been suggested (Ludlow et al., 2017). Therefore, ion channels comprising TRPC1/4/5 proteins are an important target of EA and might be a platform for developing novel anti-cancer agents (Gaunt et al., 2016, Wu et al., 2017). However, obstacles to a therapeutic strategy include metabolic instability and in vivo toxicity (Carson et al., 2015). A potential route to overcoming such obstacles is a better understanding of the structure-activity relationships of EA at TRPC1/4/5 channels. To this end, we have sought chemical elaboration of EA. Here we report on a novel EA analogue and suggest that it is a competitive antagonist with partial agonist capability.

Methods

Cell Culture

Human embryonic kidney 293 cells (HEK-293 cells) stably expressing human TRPC5 or human TRPC4β (tetracycline inducible promoter) were cultured at 37 °C in a humidified atmosphere

containing 5% CO_2 / 95% air. The HEK-293 were from Invitrogen (T-REx™, Tetracycline-Regulated Expression cell line stably expressing tetracycline (Tet) repressor). To induce the channel expression, tetracycline (1 μg mL^{-1}) was added to the cells at least 24 hours before the experiment. Dulbecco's modified Eagle medium-F12 GlutaMAX (Invitrogen, Paisley, UK) was used with supplementation of 10% fetal bovine serum (FBS) and 5% with penicillin-streptomycin (10,000 units and 10 mg streptomycin per mL in 0.9% NaCl, sigma). The cell culture medium was supplemented with the selection antibiotics blasticidin (5 μg mL^{-1}) and phleomycin (400 μg mL-1, Zeocin) (Invitrogen). The culture medium was changed every 3-4 days until the cells were 70 - 80% confluent. The cells were used at passages 5 to 20 and the same seeding conditions were maintained between experiments. A-498 renal cell carcinoma cells were from DSMZ (The Leibniz-Institute–Deutsche Sammlung von Mikroorganismen und Zellkulturen GmbH, Germany). These cells were originally established from the kidney carcinoma of a 52-year-old man in 1973. A498 were cultured in Minimum Essential Medium (MEM) Eagle medium with EBSS, L-glutamine, 2.2 g L^{-1} $NaHCO_3$ (PAN-biotech, Germany) supplemented with 5% sodium pyruvate.

Intracellular Calcium Measurement

HEK-293 or A498 cells were plated at 90% confluence in microplates (96-well plates) and incubated overnight at 37 °C, 5% CO_2. For HEK-293 cells clear-bottomed poly-D-lysine-coated black plates (Corning Life Sciences, Lowell, MA) and for A498 cells, clear-bottomed Nunc plates (Thermo Scientific) were used. The cells were illuminated with alternating 340/380 nm excitation light for fura-2 fluorescence measurements. Fluorescence emission was measured at 510 nm. In more detail, the cells were incubated for 1 hr with fura-2-AM (2 μM) in Standard Bath Solution (SBS) at 37 ºC in the presence of 0.01% pluronic acid. The fura-2 fluorescence was recorded using a 96-well fluorescence plate reader and the excitation wavelengths of 340 and 380 nm (FlexStation II384, Molecular Devices, Sunnyvale, CA, USA). Ca^{2+} was indicated by the ratio of the fluorescence (F) emission intensities for the two excitation wavelengths. Measurements were made at room temperature (21 ± 3 ºC).

Patch-clamp recording

Conventional whole-cell configuration was performed under voltage clamp at room temperature using 3–6-megaohm patch pipettes fabricated from borosilicate glass capillaries with an outside diameter of 1 mm and an inside diameter of 0.58 mm (Harvard Apparatus). The currents were recorded using an Axopatch 200B amplifier, digitized by a Digidata 1440, and recorded to a computer using pCLAMP10 (Molecular Devices). The data were filtered at 1 kHz and analyzed off-line using Clampfit software (version 10.2, Molecular Devices) and Origin software version 9.1 (OriginLab, Northampton, MA). The bath solution was SBS, and the pipette solution (intracellular solution) contained 145 mM CsCl, 2 mM $MgCl_2$, 10 mM Hepes, 1 mM EGTA (free acid), 5 mM ATP (sodium salt), and 0.1 mM GTP (sodium salt), titrated to pH 7.2 with CsOH. Cells were plated 24 h previously on glass coverslips at a low density of 20–30% and induced with tetracycline (1 μg/ml).

Chemical Synthesis

The synthesis of ether derivative A54 (**1** in Fig. S1) commenced from alcohol 2, which is readily accessible in two steps (Supporting information) from a key intermediate of previous englerin syntheses (Radtke et al., 2011, Willot et al., 2009). An iridium catalyzed etherification of alcohol 2 gave vinyl ether 3 in 82% yield (Okimoto et al., 2002). Subsequent hydroboration afforded the

glycol ether 4 in 81% yield (Hoveyda et al., 2011). The primary hydroxyl was protected as silyl ether 5 in 77% yield, followed by hydrogenolytic cleavage of benzyl ether to give alcohol 6. Finally, Yamaguchi esterification with cinnamic acid afforded ester 7 (78% yield) which was treated with tetra-*N*-butylammonium fluoride (TBAF) to give the target molecule 1 in 99% yield (Inanaga et al., 1979, Kawanami et al., 1981).

Reagents

(-)-EA and A54 were stored in aliquots at -80°C. A54 stock and working solutions were prepared similarly to those of (-)-EA, as previously described (Akbulut et al., 2015). The (-)-EA analogues were diluted to a final concentration using the standard bath solution (SBS) containing 0.1% DMSO and 0.01% pluronic acid. The SBS, which was the experimental buffer, contained (mM): NaCl 135, KCl 5, $MgCl_2$ 1.2, $CaCl_2$ 1.5, glucose 8 and Hepes 10 (pH titrated to 7.4 using NaOH).

Data Analysis

All data are presented as means ± standard error of the mean (SEM) and $P < 0.05$ considered statistically significant after Two-Sample Test (t-test) for comparisons of two independent groups or ANOVA (One-Way, and post test Bonferroni) for multiple groups (post hoc test was only applied when ANOVA gave $P < 0.05$). Origin 9.1 software was used to analyse the results. In Ca^{2+} studies, the half maximal inhibitory concentration (IC_{50}) was obtained by normalizing to the maximal response of (-)-Englerin A and the curves were fitted in Origin 9.1 software using $y = START + (END - START) * x^n / (k^n + x^n)$, where y is the Ca^{2+} concentration (reflected by fura-2 ratio), x the concentration of the compound, k the IC_{50} or EC_{50}, and n the number of binding site per target molecule. The rate of rise of the Ca^{2+} signal in response to Gd^{3+} was fitted in Origin 9.1 using $y = A1*\exp(-x/t1) + y0$, where y is Ca^{2+}, x time, A1 the maximum response, y0 the Ca^{2+} at the time of Gd^{3+} application, and t1 the time constant. The data in all experiments are represented as n/N, where n indicates independent experiments and N indicates replicates in columns of the 96-well plate. Statistical significance is indicated by * ($P < 0.05$).

Results

Structures of (-)-Englerin A (EA), Englerin B (EB) and Analogue 54 (A54)

EA and its inactive metabolite EB (Fig. 1A, B) were used to guide the generation of analogues which might be active at endogenous TRPC4/5-containing channels. In this article we show the structure and data for only one of these analogues, A54 (Fig. 1C). Synthesis routes and chemical validation are provided (Supplementary Fig. S1).

A54 lacks agonist activity but inhibits EA-evoked Ca^{2+} entry in A498 cells

To test the functionality of EA and its analogues we first used intracellular Ca^{2+} measurement in the A498 cells which express endogenous EA-responsive TRPC4/TRPC1 heteromeric channels (Akbulut et al., 2015, Ludlow et al., 2017). Initially, a single concentration of each compound was tested. As expected, EA was effective and EB ineffective (Fig. 2A, B). Like EB, A54 failed to evoke a Ca^{2+} signal and therefore appeared to be inactive (Fig. 2A, B). Nevertheless, we also tested if A54 could affect the response to EA. A498 cells were pre-incubated with 1 µM A54 for 30 min and then 100 nM EA was tested in the continuous presence of A54 (Fig. 2C). Strikingly, A54

abolished the EA response (Fig. 2C). In contrast, EB failed to affect the EA response (Fig. 2C). We next constructed a concentration-response curve for A54 against the EA response, pre-incubating A498 cells with A54 at a range of concentrations (1-1000 nM) for 30 min and then testing EA (Fig. 2D). A54 was a potent inhibitor of the EA response, causing 50% inhibition at 62 nM (Fig. 2D, E). The data suggest that A54, unlike EB, is an antagonist of EA.

EA-dependent inhibition of TRPC5 channels by A54

To gain insight into the mechanism of inhibition by A54 we switched to studying HEK 293 cells which contain tetracycline-inducible expression of human TRPC5, generating TRPC5 homomeric channels. These cells exhibit not only TRPC5 activity evoked by EA but also robust, albeit smaller, TRPC5 activity evoked by gadolinium ions (Gd^{3+}) (Akbulut et al., 2015, Ludlow et al., 2017, Naylor et al., 2016) (Fig. 3A). We could, therefore, test A54 against two different modes of channel activity to determine if the effect of A54 had specificity for the EA response. EA evoked a large Ca^{2+} response in the TRPC5-expressing cells and, as expected, this effect was abolished by A54 (Fig. 3A, B). A54 did not however inhibit the Gd^{3+} response, but enhanced its amplitude and rate of onset (Fig. 3A, C, D).

To further investigate the dual effect of A54 we used whole-cell patch-clamp. EA activated TRPC5-mediated current as expected (Fig. 4A, B). Addition of A54 in the continuous presence of EA caused striking inhibition of the EA-evoked current (Fig. 4A-D) and this effect was reversible on wash-out of A54 (Fig. 4A, B). The channels could also be activated by Gd^{3+} but in this case A54 further enhanced the current (Fig. 5A-D). The data suggest that the inhibitory effect of A54 is EA-dependent and that, in the absence of EA, A54 has a sharply contrasting positive effect on the Gd^{3+} response.

A54 behaves like a competitive antagonist of EA at TRPC5 channels

Because the inhibitory effect of A54 is EA-dependent we considered whether it might bind part of the same site as EA and thus compete with EA. To test this hypothesis, we constructed concentration-response curves for EA in the absence of A54 and in the presence of two different concentrations of A54 (10 and 50 nM) (Fig. 6A-C). The inhibition by A54 was surmountable and increasing concentrations of A54 caused parallel rightward shifts in the EA concentration-response curve (Fig. 6D). Schild analysis revealed a slope close to unity (Fig. 6E). EA responses reached steady-state for most concentrations of EA but the slowness of the response to low concentrations of EA meant that the responses fell short of steady-state in some instances. We accepted this weakness because of concern about the health of cells when long exposures to EA were used. The data suggest that A54 is a competitive antagonist of EA at TRPC5 channels.

A54 is a weak antagonist of EA at TRPC4 channels

We next investigated the effect of A54 on TRPC4 homomeric channels overexpressed in HEK 293 cells. Unexpectedly, A54 was only a mild antagonist of EA at TRPC4 channels (Fig. 7A, B) and furthermore A54 lacked agonist activity on TRPC4 channels (Fig. 7C). The data suggest that the EA binding site associated with TRPC4 channels does not bind A54 efficiently or that A54 binds

tightly but does not compete effectively with EA. These findings contrast with TRPC5 channels and native TRPC4/TRPC1 channels.

A54 strongly potentiates S1P-evoked TRPC4 activity

To further investigate the relationship between A54 and TRPC4 channels we used a physiological agonist, S1P, which activates TRPC4 channels via G protein signaling. Strikingly, A54 markedly potentiated S1P-evoked Ca^{2+} entry through TRPC4 channels (Fig. 7C, D). The data suggest that A54 is an enhancer of TRPC4 channel activity evoked by S1P.

A54 has no effect on TRPC3 channels

EA appears to be selective for TRPC1/4/5 channels, lacking effect on 13 other ion channels investigated including TRPC3, a member of the TRPC3/TRPC6/TRPC7 subfamily of TRPC channels (Akbulut et al., 2015). Here we investigated if there was effect of A54 on TRPC3 homomeric channels overexpressed in HEK 293 cells. A54 (1 μM) did not activate TRPC3 or inhibit or potentiate TRPC3-mediated Ca^{2+} entry activated by the TRPC3 agonist 1-oleoyl-2-acetylglycerol (OAG) (Fig. 8A, B). The data suggest that A54 has no effect on TRPC3 channels.

Discussion and conclusions

The study reveals how subtle chemical elaboration of EA can lead to a compound (A54) which is a potent antagonist of EA at TRPC5 homomeric channels and endogenous TRPC4/TRPC1-containing channels, yet not a general blocker of the channels. The antagonism had characteristics of surmountable competitive antagonism at TRPC5 channels, suggesting that A54 interacts at the same site as EA but is not able to trigger channel opening. Strikingly, however, A54 was a strong enhancer of TRPC5 channel activity which had already been induced by Gd^{3+} and TRPC4 channel activity induced by S1P. A54 is therefore capable of antagonist and enhancer (facilitating) activity; i.e. it is not a pure antagonist but retains some agonist-like (enhancer) capability in the presence of a co-factor (Gd^{3+} or S1P).

The existence and location of a binding site for EA is unknown but its ability to robustly activate TRPC4 channels in excised membrane patches even in the complete absence of exogenous co-factors is suggestive of an agonist binding site on the channel protein itself (Akbulut et al., 2015). This site is either on the extracellular surface of the channels or only accessible via the outer leaflet of the bilayer because EA only activates the channels when applied to the outer and not inner surface of the membrane (Akbulut et al., 2015). By implication, the A54 site would also be on the channel itself. Direct proof is however lacking.

The action of EA on TRPC1/4/5 channels is remarkable – it is much stronger and more robust as an agonist than other known activators of the channels. Therefore, there would seem not only to be an EA binding site on the channels but also the very efficient coupling of this binding site to channel activation. Such a site may simply exist by chance and serve no physiological purpose, but it might alternatively serve a purpose which is not yet recognised. In this latter regard, it will be interesting to test competitive antagonists of EA (e.g. A54) in physiological studies.

As TRPC4 and TRPC5 proteins share 65% amino acid sequence, we were expecting A54 to block the TRPC4 Ca^{2+} entry evoked by EA. Surprisingly, however, 1 µM A54 had only a modest inhibitory effect (Fig. 7) compared with full inhibition at TRPC5 channels (Figs. 2 and 3). Moreover, A54 had an enhancing effect in the presence of the physiological agonist S1P, increasing the Ca^{2+} entry more than 3-fold (Fig. 7). The effect was similar to the enhancing effect of A54 at TRPC5 channels in the presence of Gd^{3+} (Figs. 3 and 5). Such effects might be explained by a conformational change in the channels (induced by S1P or Gd^{3+}) which allows A54 to access an efficacy (agonist) site. Therefore, the EA and A54 data could be explained by the existence of two binding sites which are in close physical proximity: Site 1 allowing binding without efficacy, and Site 2 allowing binding and efficacy. In this model, EA would bind Sites 1 and 2 (and therefore have direct agonist effect), while A54 would bind only Site 1 in the absence of a co-factor (and therefore antagonise EA) but also Site 2 in the presence of the co-factor (and therefore have an enhancing effect).

In conclusion, the study has revealed a new tool compound for EA and TRPC1/4/5 channel research and, to the best of our knowledge, the first known competitive antagonist of EA. This was achieved by minimal structural modification to EA. It is not a perfect antagonist because it has enhancer capability in the presence of a co-factor (Gd^{3+} at TRPC5 channels and S1P at TRPC4 channels) but it shows impressive capability as a surmountable competitive antagonist when used in isolation in the low to middle nanomolar concentration range. The compound should facilitate studies aimed at better understanding TRPC1/4/5 channel activation, TRPC1/4/5 channel binding sites, and the physiological relevance of the action of EA. Because of the in vivo toxicity of EA (Carson et al, 2015), such a competitive antagonist might also have use as an antidote to EA poisoning.

Acknowledgements
This work was supported by the University of Leeds, the Max Planck Society (MPG) and The Lead Discovery Center (LDC).

Conflict of interest
The authors state no conflict of interest.

Author contributions
H.N.R. performed the research (cell culture, calcium measurements, patch-clamp electrophysiology) designed the research study, contributed intellectually, analysed the data, generated the figures and wrote the manuscript with D.J.B.. M.C. led the chemical synthesis of A54. H.W., B.K., A.C., M.C., T.S., S.H., P.N. and D.J.B. performed or advised on chemical synthesis and usage, generated research funds and ideas, led and coordinated the project, or interpreted data.

References

Abramowitz J & Birnbaumer L (2009). Physiology and pathophysiology of canonical transient receptor potential channels. FASEB J, 23: 297-328.

Akbulut Y, Gaunt HJ, Muraki K, Ludlow MJ, Amer MS, Bruns A, Vasudev NS, Radtke L, Willot M, Hahn S, Seitz T, Ziegler S, Christmann M, Beech DJ & Waldmann H (2015). (-)-Englerin A is a potent and selective activator of TRPC4 and TRPC5 calcium channels. Angew Chem Int Ed Engl, 54: 3787-91.

Beech DJ (2013). Characteristics of transient receptor potential canonical calcium-permeable channels and their relevance to vascular physiology and disease. Circ J, 77: 570-9.

Bon RS & Beech DJ (2013). In pursuit of small molecule chemistry for calcium-permeable non-selective TRPC channels -- mirage or pot of gold? Br J Pharmacol, 170: 459-74.

Caropreso V, Darvishi E, Turbyville TJ, Ratnayake R, Grohar PJ, Mcmahon JB & Woldemichael GM (2016). Englerin A Inhibits EWS-FLI1 DNA Binding in Ewing Sarcoma Cells. J Biol Chem, 291: 10058-66.

Carson C, Raman P, Tullai J, Xu L, Henault M, Thomas E, Yeola S, Lao J, Mcpate M, Verkuyl JM, Marsh G, Sarber J, Amaral A, Bailey S, Lubicka D, Pham H, Miranda N, Ding J, Tang HM, Ju H, Tranter P, Ji N, Krastel P, Jain RK, Schumacher AM, Loureiro JJ, George E, Berellini G, Ross NT, Bushell SM, Erdemli G & Solomon JM (2015). Englerin A Agonizes the TRPC4/C5 Cation Channels to Inhibit Tumor Cell Line Proliferation. PLoS One, 10: e0127498.

Damann N, Voets T & Nilius B (2008). TRPs in our senses. Curr Biol, 18: R880-9.

Gaunt HJ, Vasudev NS & Beech DJ (2016). Transient receptor potential canonical 4 and 5 proteins as targets in cancer therapeutics. Eur Biophys J, 45: 611-620.

Hoveyda HR, Marsault E, Gagnon R, Mathieu AP, Vezina M, Landry A, Wang Z, Benakli K, Beaubien S, Saint-Louis C, Brassard M, Pinault JF, Ouellet L, Bhat S, Ramaseshan M, Peng X, Foucher L, Beauchemin S, Bherer P, Veber DF, Peterson ML & Fraser GL (2011). Optimization of the potency and pharmacokinetic properties of a macrocyclic ghrelin receptor agonist (Part I): Development of ulimorelin (TZP-101) from hit to clinic. J Med Chem, 54: 8305-20.

Inanaga J, Hirata K, Saeki H, Katsuki T & Yamaguchi M (1979). A rapid esterification by means of mixed anhydride and its application to large-ring lactonization. Bulletin of the chemical society of Japan, 52: 1989-1993.

Kawanami Y, Dainobu Y, Inanaga J, Katsuki T & Yamaguchi M (1981). Synthesis of thiol esters by carboxylic trichlorobenzoic anhydrides. Bulletin of The Chemical Society of Japan, 54: 943-944.

Ludlow MJ, Gaunt HJ, Rubaiy HN, Musialowski KE, Blythe NM, Vasudev NS, Muraki K & Beech DJ (2017). (-)-Englerin A-evoked Cytotoxicity Is Mediated by Na+ Influx and Counteracted by Na+/K+-ATPase. J Biol Chem, 292: 723-731.

Ma X, Cai Y, He D, Zou C, Zhang P, Lo CY, Xu Z, Chan FL, Yu S, Chen Y, Zhu R, Lei J, Jin J & Yao X (2012). Transient receptor potential channel TRPC5 is essential for P-glycoprotein induction in drug-resistant cancer cells. Proc Natl Acad Sci U S A, 109: 16282-7.

Maier T, Follmann M, Hessler G, Kleemann HW, Hachtel S, Fuchs B, Weissmann N, Linz W, Schmidt T, Lohn M, Schroeter K, Wang L, Rutten H & Strubing C (2015). Discovery and pharmacological characterization of a novel potent inhibitor of diacylglycerol-sensitive TRPC cation channels. Br J Pharmacol, 172: 3650-60.

Miller M, Wu M, Xu J, Weaver D, Li M & Zhu MX (2011). High-Throughput Screening of TRPC Channel Ligands Using Cell-Based Assays. In: ZHU, M. X. (ed.) TRP Channels. Boca Raton (FL).

Moran MM, Mcalexander MA, Biro T & Szallasi A (2011). Transient receptor potential channels as therapeutic targets. Nat Rev Drug Discov, 10: 601-20.

Naylor J, Minard A, Gaunt HJ, Amer MS, Wilson LA, Migliore M, Cheung SY, Rubaiy HN, Blythe NM, Musialowski KE, Ludlow MJ, Evans WD, Green BL, Yang H, You Y, Li J, Fishwick CW, Muraki K, Beech DJ & Bon RS (2016). Natural and synthetic flavonoid modulation of TRPC5 channels. Br J Pharmacol, 173: 562-74.

Okimoto Y, Sakaguchi S & Ishii Y (2002). Development of a highly efficient catalytic method for synthesis of vinyl ethers. J Am Chem Soc, 124: 1590-1.

Radtke L, Willot M, Sun H, Ziegler S, Sauerland S, Strohmann C, Frohlich R, Habenberger P, Waldmann H & Christmann M (2011). Total synthesis and biological evaluation of (-)-englerin A and B: synthesis of analogues with improved activity profile. Angew Chem Int Ed Engl, 50: 3998-4002.

Ratnayake R, Covell D, Ransom TT, Gustafson KR & Beutler JA (2009). Englerin A, a selective inhibitor of renal cancer cell growth, from Phyllanthus engleri. Org Lett, 11: 57-60.

Rubaiy HN (2017). A Short Guide to Electrophysiology and Ion Channels Journal of Pharmacy and Pharmaceutical Sciences, 20: 48-67.

Rubaiy HN, Ludlow MJ, Bon RS & Beech DJ (2017a). Pico145 - powerful new tool for TRPC1/4/5 channels. Channels (Austin): 1-3.

Rubaiy HN, Ludlow MJ, Henrot M, Gaunt HJ, Miteva K, Cheung SY, Tanahashi Y, Hamzah N, Musialowski KE, Blythe NM, Appleby HL, Bailey MA, Mckeown L, Taylor R, Foster R, Waldmann H, Nussbaumer P, Christmann M, Bon RS, Muraki K & Beech DJ (2017b). Picomolar, selective and subtype specific small-molecule inhibition of TRPC1/4/5 channels. J Biol Chem.

Sourbier C, Scroggins BT, Ratnayake R, Prince TL, Lee S, Lee MJ, Nagy PL, Lee YH, Trepel JB, Beutler JA, Linehan WM & Neckers L (2013). Englerin A stimulates PKCtheta to inhibit insulin signaling and to simultaneously activate HSF1: pharmacologically induced synthetic lethality. Cancer Cell, 23: 228-37.

Washburn DG, Holt DA, Dodson J, Mcatee JJ, Terrell LR, Barton L, Manns S, Waszkiewicz A, Pritchard C, Gillie DJ, Morrow DM, Davenport EA, Lozinskaya IM, Guss J, Basilla JB, Negron LK, Klein M, Willette RN, Fries RE, Jensen TC, Xu X, Schnackenberg CG & Marino JP, Jr. (2013). The discovery of potent blockers of the canonical transient receptor channels, TRPC3 and TRPC6, based on an anilino-thiazole pharmacophore. Bioorg Med Chem Lett, 23: 4979-84.

Willot M, Radtke L, Konning D, Frohlich R, Gessner VH, Strohmann C & Christmann M (2009). Total synthesis and absolute configuration of the guaiane sesquiterpene englerin A. Angew Chem Int Ed Engl, 48: 9105-8.

Wu Z, Zhao S, Fash DM, Li Z, Chain WJ & Beutler JA (2017). Englerins: A Comprehensive Review. J Nat Prod, 80: 771-781.

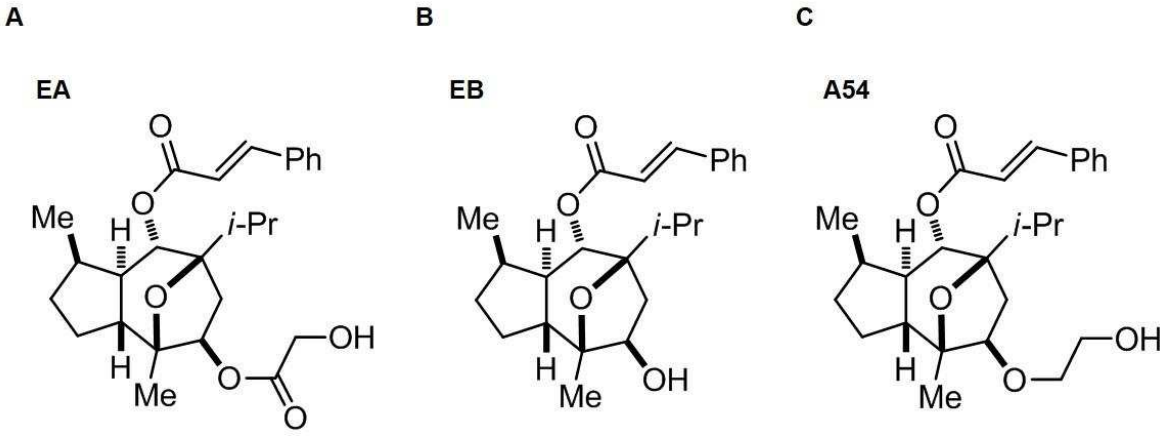

Figure 1. Structures of (-)-Englerin A (EA), Englerin B (EB) and Analogue A54.

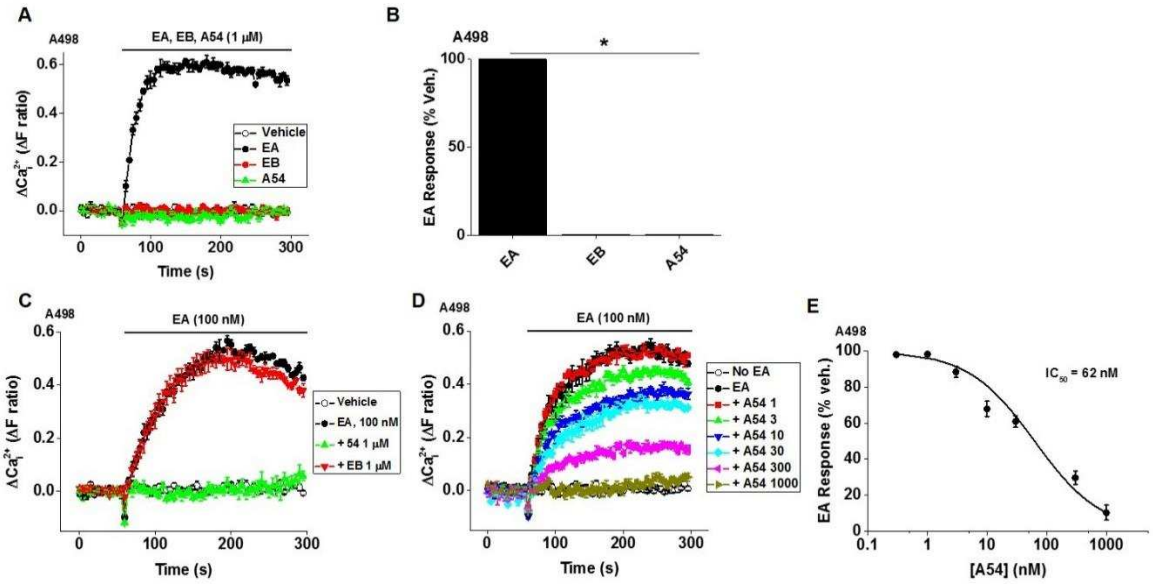

Figure 2. Activity of (-)-Englerin A (EA), Englerin B (EB) and analogue 54 (A54) in A498 cells. (A) Representative Ca^{2+} measurement data from a single 96-well plate showing the EA-evoked Ca^{2+} entry (black circles) and lack of effect of EB (red circle) or A54 (green triangle) in A498 cells. (B) Summary data for experiments of the same type (A) plotted as a percentage of the maximum EA response and expressed as percentages (n/N = 7/21, one-way ANOVA and post-test Bonferroni). (C) Representative traces showing 1 μM of A54 (green) was sufficient to inhibit activation by EA (100 nM) whereas 1 μM EB lacked effect (red). (D) Example concentration-dependent inhibition traces of 100 nM EA responses by A54 at increasing concentrations (numbers 1-1000 indicate concentrations in nM). (E) Concentration-response data for inhibition of EA responses by A54 fitted with the Hill equation (IC_{50} = 62 ± 17 nM, slope = 0.8 ± 0.01) (n/N = 5/15, mean ± SEM).

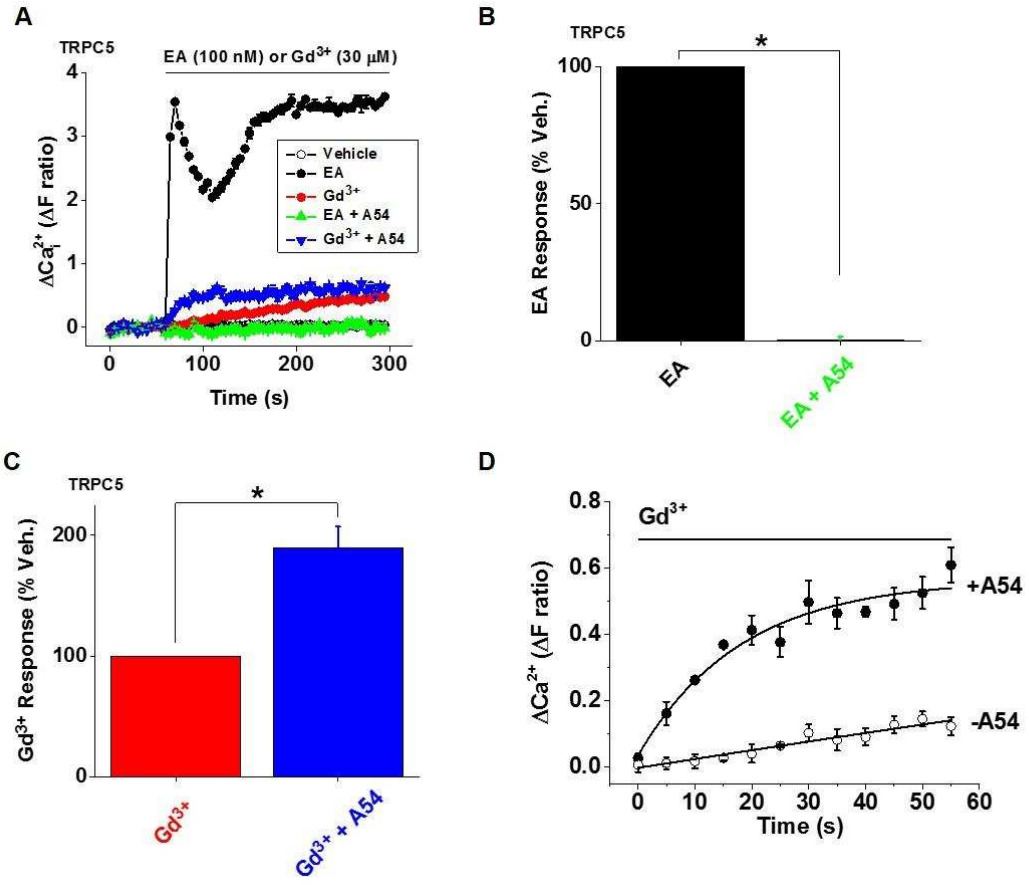

Figure 3. A54 inhibits EA but not Gd^{3+}-evoked TRPC5 channel activity. Intracellular Ca^{2+} responses in HEK-TRPC5 cells to EA (100 nM, black) and Gd^{3+} (30 µM, red) in the absence and presence of 1 µM A54 (A). (B) For EA experiments of the type illustrated in (A), mean ± standard error of the mean data normalized to the vehicle control for A54 (n/N = 8/32). (C) For Gd^{3+} experiments of the type illustrated in (A), mean ± standard error of the mean data normalized to the vehicle control for A54 (n/N = 8/32). The time-point at which the amplitude of the Gd^{3+} response was measurement was from 150 to 200 seconds. (D) Activation time-course of Gd^{3+} responses in the absence and presence of A54. The curves were fitted exponential functions with time constants of 780 ± 7.6 s (Gd^{3+} -A54) and 18.1 ± 3.9 s (Gd^{3+} +A54) (n/N = 8/32).

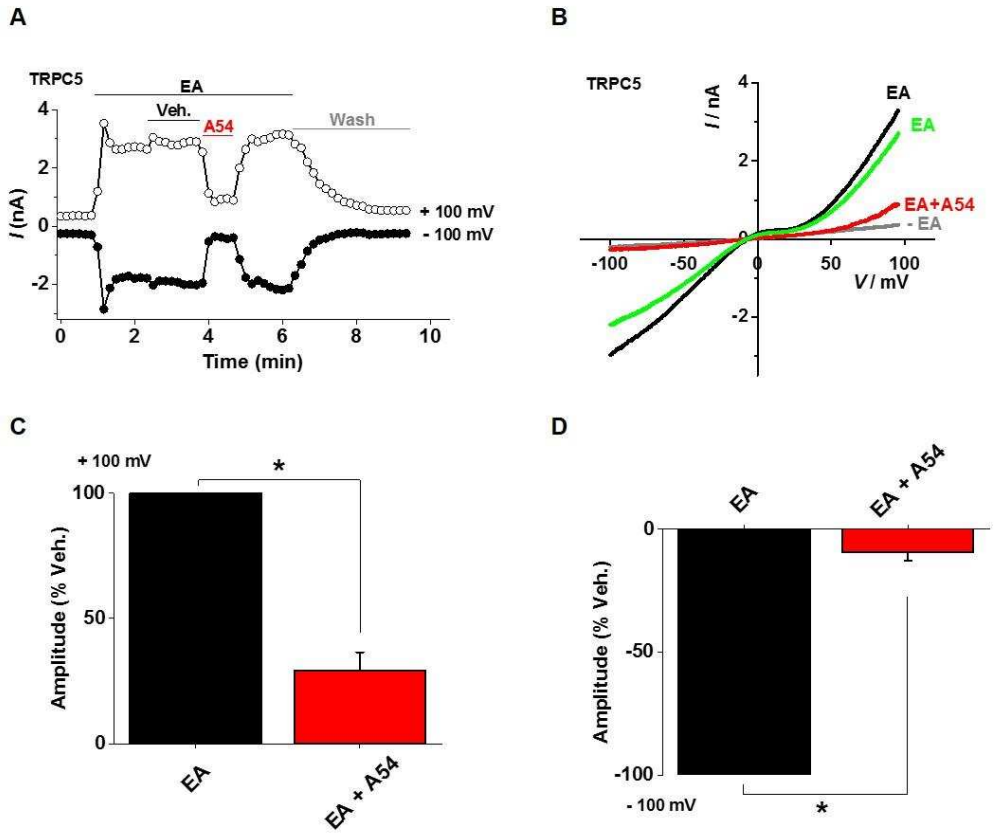

Figure 4. A54 inhibits EA-evoked current in TRPC5 channels. (A) Example whole cell patch clamp data from a TRPC5-expressing HEK 293 cell showing current sampled at -100 and +100 mV during ramp changes in voltages (all agents were bath-applied). 10 nM EA and 1 µM A54 were used. Vehicle (Veh.) was DMSO. Wash indicates wash-out of EA and A54. (B) Representative current-voltage relationship (IVs) from experiments of the type illustrated in (A). (C, D) Mean percentage inhibition responses to A54 as illustrated in (A) for +100 mV (C) and -100 mV (D) (n = 5 independent recordings).

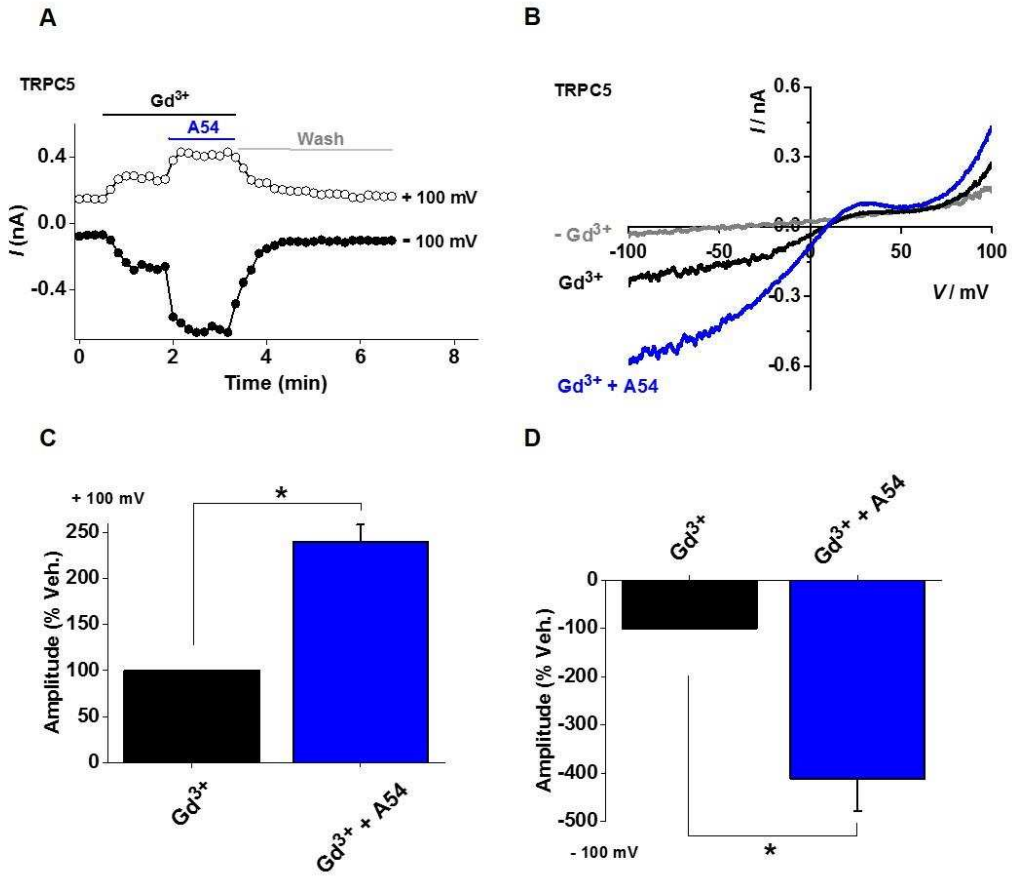

Figure 5. A54 enhances Gd^{3+}-evoked current in TRPC5 channels. (A) Example whole cell patch clamp data from a TRPC5-expressing HEK 293 cell showing current sampled at -100 and +100 mV during ramp changes in voltages (all agents were bath-applied). 3 µM Gd^{3+} and 1 µM A54 were used. Wash indicates wash-out of Gd^{3+} and A54. (B) Representative current-voltage relationship (IVs) from experiments of the type illustrated in (A). (C, D) Mean percentage enhancing responses to A54 as illustrated in (A) for +100 mV (C) and -100 mV (D) (n = 5 independent recordings).

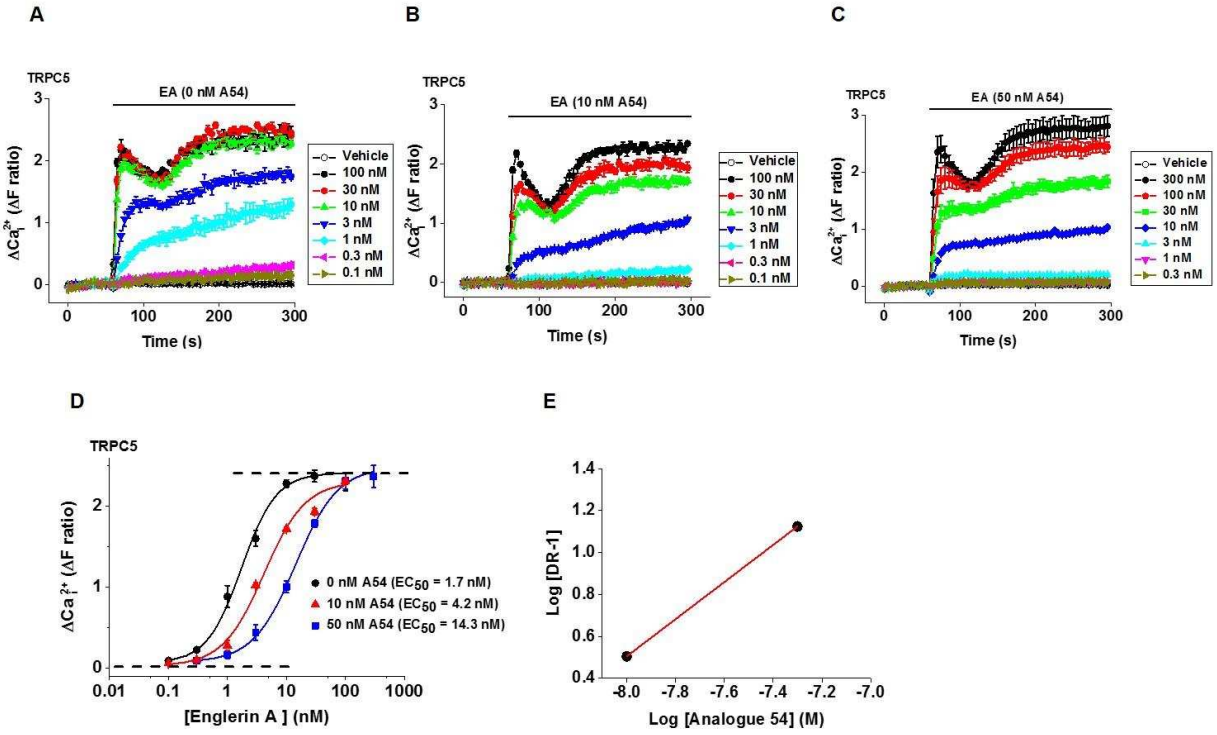

Figure 6. A54 causes parallel rightward shifts of the EA concentration-response curve. (A-C) Example data from HEK-TRPC5 cells showing concentration-dependence of EA responses in the presence of 0 nM (A), 10 nM (B) and 50 nM (C) A54. (D) Mean ± SEM concentration-response data for experiments of the type illustrated in (A-C) (n/N = 6/24 for 0 and 50 nM and n/N = 5/16 for 10 nM). EA EC_{50}s were 1.7 nM (0 nM A54), 4.2 nM (10 nM A54) and 14.3 nM (50 nM A54). EA slope values were 1.4 (0 nM A54), 1.3 (10 nM A54), and 1.3 (50 nM A54). (E) Schild plot regression analysis with a slope near 1 (0.9) indicating that A54 is a competitive antagonist (DR in Y axis indicates the dose ratio).

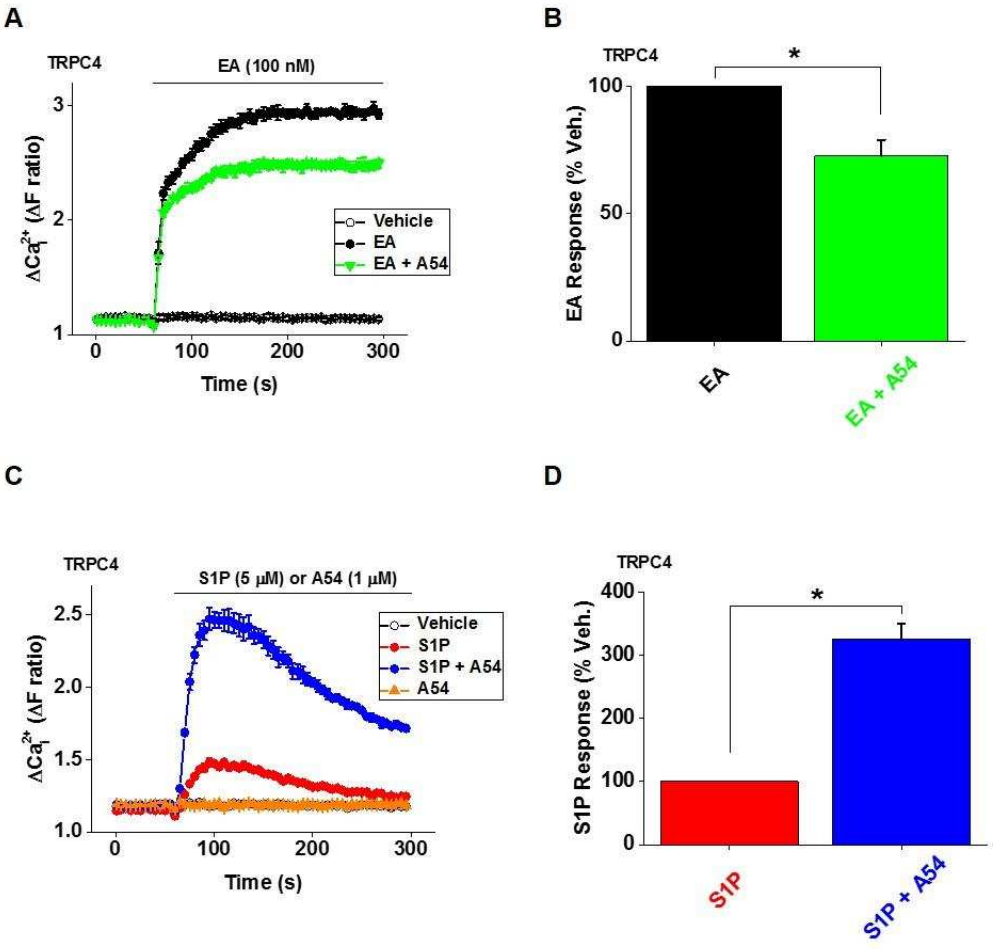

Figure 7. A54 is a striking enhancer of S1P-evoked TRPC4 channel activity. (A) Intracellular Ca^{2+} responses in HEK-TRPC4 cells to EA (100 nM, black) in the absence and presence (green) of 1 µM A54. (B) Mean ± standard error of the mean data normalized to the vehicle control for A54 of the type illustrated in (A) (n/N = 5/15 for all data). (C) Intracellular Ca^{2+} responses in HEK-TRPC4 cells to A54 (1 µM, orange) and S1P (5 µM, red) in the absence and presence (blue) of 1 µM A54. (D) Mean ± standard error of the S1P mean data normalized to the vehicle control for A54 of the type illustrated in (C), (n/N = 5/15 for all data).

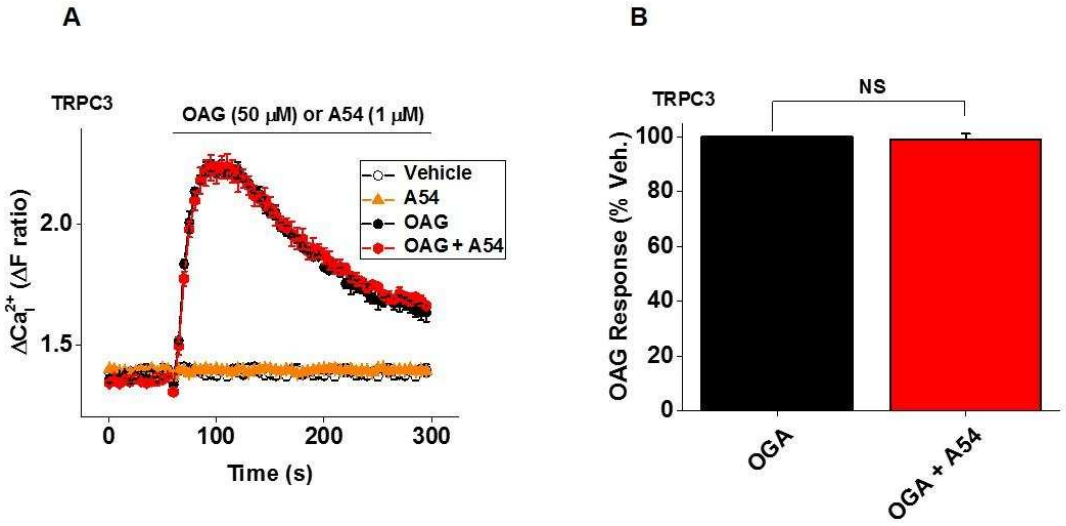

Figure 8. Lack of effect of A54 on TRPC3 channel activity. (A) Intracellular Ca^{2+} responses to A54 (1 µM, orange) and 1-oleoyl-2-acetyl-snglycerol (OAG, 50 µM, black) in the absence and presence (red) of 1 µM A54 in HEK 293 Tet^+ cell lines stably expressing human TRPC3 (n/N = 6/18). (B) Mean ± standard error of the mean data normalized to the vehicle control for A54 of the type illustrated in (A) (n/N = 6/18).

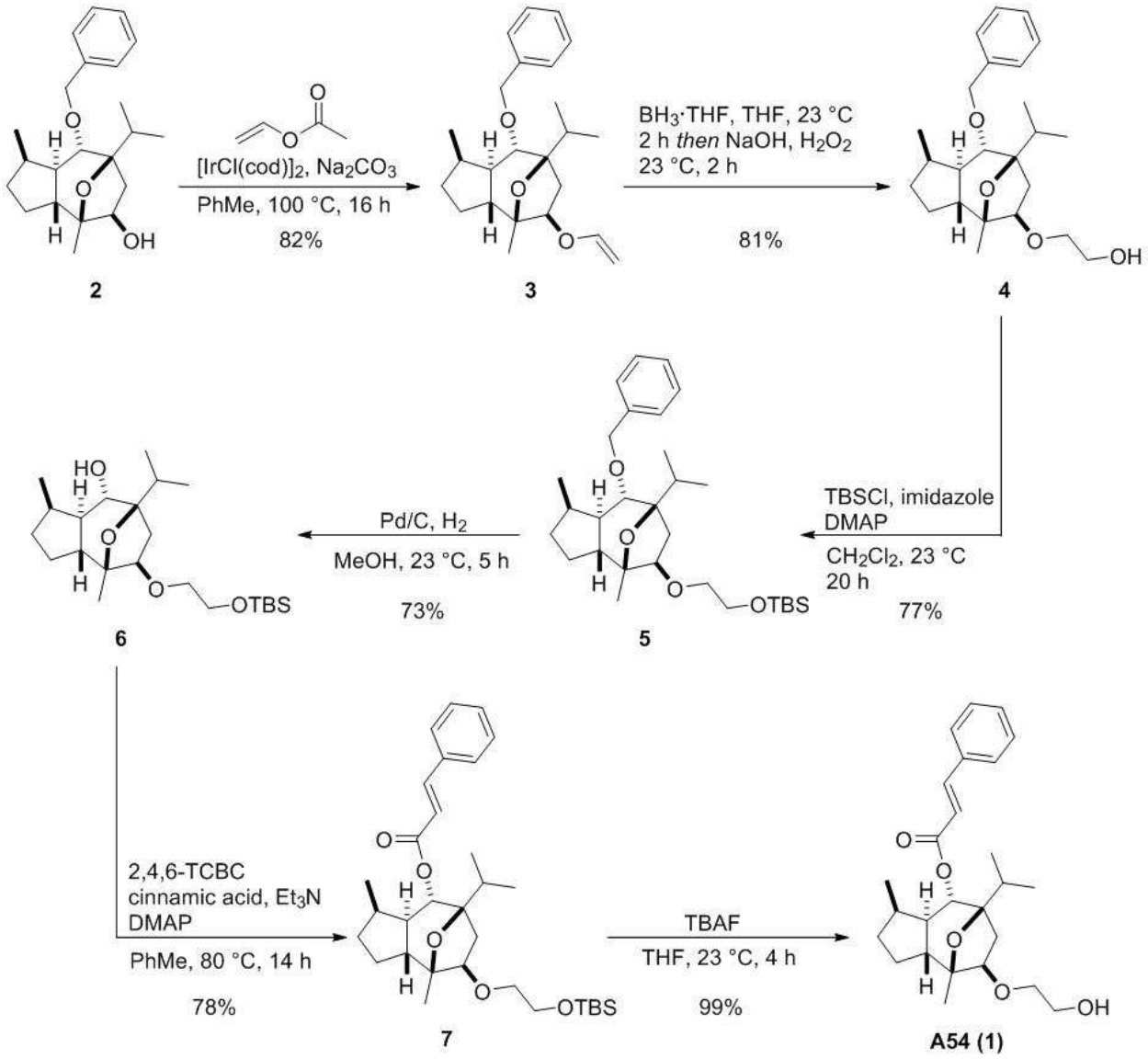

Supplementary Figure S1. Chemical synthesis and validation of analogue A54 (1).

Supporting Information

Identification of an (-)-Englerin A analogue which antagonizes (-)-Englerin A at TRPC1/4/5 channels

General Information

^{1}H and ^{13}C NMR spectral data were recorded at 400/500/700 MHz (^{1}H) and 101/126/176 MHz (^{13}C) on a JEOL ECX400 spectrometer/ JEOL ECP500 spectrometer/ BRUKER AVANCE500 spectrometer/ Bruker AVANCE700 spectrometer. The chemical shifts were referenced to the corresponding residual solvent signal ($CDCl_3$: δ_H = 7.26 ppm, δ_C = 77.16 ppm). IR spectra were measured on a Jasco FT/IR-4100 equipped with an ATR unit. All IR spectra were measured with neat substances. High resolution ESI-TOF mass spectra were measured on an Agilent 6210-System. Optical rotation values were measured on a Jasco P-2000 polarimeter. Products were purified by flash chromatography on silica gel 300-400 mesh (Macherey & Nagel). Unless otherwise indicated, all reagents were purchased from commercial distributors and used without further purification. Dry THF, dry PhMe and dry CH_2Cl_2 were purified over a MBRAUN MB SPS-800 system from HPLC grade solvents.

(((1R,3aR,4S,5R,7R,8S,8aR)-8-(benzyloxy)-7-isopropyl-1,4-dimethyldecahydro-4,7-epoxyazulen-5-yl)oxy)(tert-butyl)dimethylsilane (B)

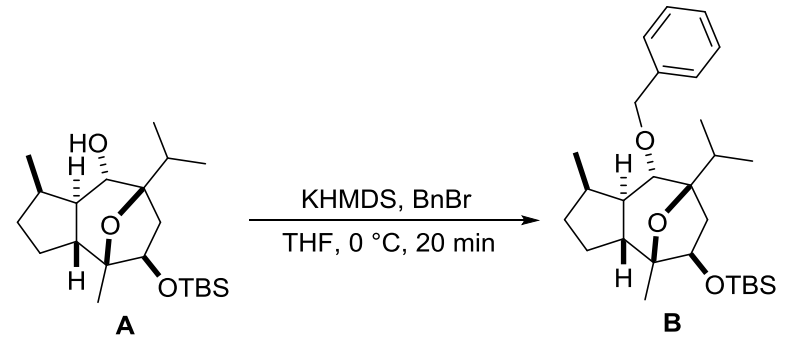

A $C_{21}H_{40}O_3Si$ (368.63)

B $C_{28}H_{46}O_3Si$ (458.76)

An oven-dried 10 mL round-bottom-flask equipped with a Teflon-coated magnetic stirring bar was charged with alcohol **A** (100 mg, 271 µmol, 1.00 equiv) and dry THF (2.7 mL) under an argon atmosphere. The solution was cooled to 0 °C and KHMDS (1M in THF) (1.40 mL, 1.36 mmol, 5.00 equiv) was added dropwise. Then benzyl bromide (161 µL, 1.36 mmol, 5.00 equiv) was added and the reaction was stirred for additional 20 min. The reaction was quenched by adding 1M HCl solution (10 mL) and extracted with Et_2O (4 × 2 mL). The combined organic phases were dried over sodium sulfate and the solvent was removed under reduced pressure. The crude product was purified by flash

chromatography on silica gel (pentane–Et_2O, 50:1) to give the ether **B** (112 mg, 244 μmol, 81%) as a clear oil.

$[\alpha]_D^{20}$ −40.2 (c 1.00, $CHCl_3$), ^1H NMR (700 MHz, $CDCl_3$) δ 7.37 – 7.27 (m, 4H), 7.28 – 7.25 (m, 1H), 4.70 (d, J = 10.9 Hz, 1H), 4.59 (d, J = 11.0 Hz, 1H), 3.92 (dd, J = 7.5, 2.6 Hz, 1H), 3.47 (d, J = 9.7 Hz, 1H), 2.40 (ddd, J = 13.8, 9.1, 6.9 Hz, 2H), 2.07 (hept, J = 6.9 Hz, 1H), 1.96 (dddd, J = 13.7, 11.5, 8.1, 2.8 Hz, 1H), 1.72 – 1.59 (m, 3H), 1.39 (ddd, J = 13.2, 9.8, 6.4 Hz, 1H), 1.32 – 1.21 (m, 1H), 1.17 (s, 3H), 1.05 (d, J = 6.8 Hz, 3H), 1.04 (d, J = 7.0 Hz, 3H), 1.04 – 1.01 (m, 1H), 0.96 (d, J = 7.1 Hz, 3H), 0.89 (s, 9H), 0.03 (s, 3H), 0.02 (s, 3H) ppm. ^{13}C NMR (176 MHz, $CDCl_3$) δ 139.3, 128.4 (2C), 127.5, 127.4 (2C), 85.8, 85.4, 78.2, 73.0, 72.6, 48.1, 47.6, 42.8, 32.6, 32.0, 31.4, 25.9 (3C), 24.6, 19.9, 18.5, 18.3, 17.7, 17.6, -4.5, -4.9 ppm. IR (neat): 2955, 2929, 2857, 1471, 1461, 1380, 1253, 1086, 1066, 1022, 1005, 990, 931, 901, 862, 834, 794, 772, 733, 695 cm^{-1}. HRMS (ESI): m/z calcd for $C_{28}H_{46}O_3Si$ $[M + Na]^+$: 481.3114; found: 481.3136.

(1R,3aR,4S,5R,7R,8S,8aR)-8-(benzyloxy)-7-isopropyl-1,4-dimethyldecahydro-4,7-epoxyazulen-5-ol (2)

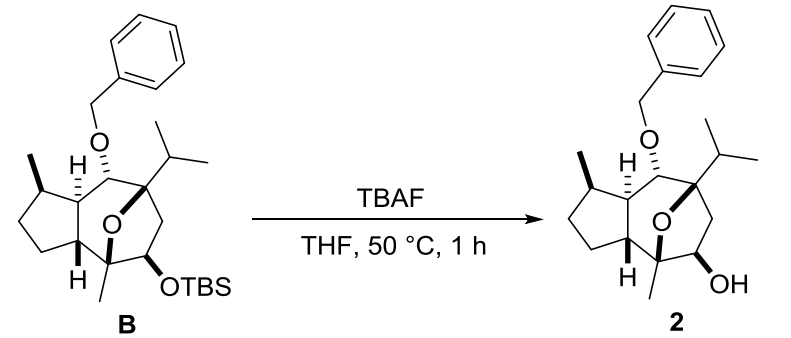

B
$C_{28}H_{46}O_3Si$ (458.76)

2
$C_{22}H_{32}O_3$ (344.50)

An oven-dried 5 mL round-bottom-flask equipped with a Teflon-coated magnetic stirring bar was charged with ether **B** (20.0 mg, 44.0 μmol, 1.00 equiv) under an argon atmosphere. TBAF solution (1M in THF) (131 μL, 131 μmol, 3.00 equiv) was added at 23 °C and the reaction was stirred at 50 °C for 1 h. The solvent was removed under reduced pressure. The crude product was purified by flash chromatography on silica gel (pentane–Et_2O, 1:1) to give the alcohol **2** (14.5 mg, 42.1 μmol, 97%) as a clear oil.

$[\alpha]_D^{20}$ −26,6 (c 1.00, $CHCl_3$), ^1H NMR (400 MHz, $CDCl_3$) δ 7.36 – 7.21 (m, 5H), 4.70 (d, J = 11.0 Hz, 1H), 4.58 (d, J = 11.0 Hz, 1H), 3.94 (td, J = 7.5, 2.5 Hz, 1H), 3.48 (d, J = 9.7 Hz, 1H), 2.54 (dd, J = 14.6, 7.6 Hz, 1H), 2.40 (sept, J = 6.6 Hz, 1H), 2.09 (hept, J = 6.9 Hz, 1H), 1.95 (dddd, J = 13.8, 11.2, 8.0, 2.7 Hz, 1H), 1.74 – 1.61 (m, 3H), 1.47 – 1.36 (m, 1H), 1.34 (d, J = 7.4 Hz, 1H), 1.31 – 1.25 (m, 1H) 1.23 (s, 3H), 1.11 – 1.06 (m, 1H), 1.05 (d, J = 6.8 Hz, 3H), 1.04 (d, J = 7.0 Hz, 3H), 0.96 (d, J = 7.1 Hz, 3H) ppm. ^{13}C NMR (126 MHz, $CDCl_3$) δ 139.1, 128.4 (2C), 127.5, 127.3 (2C), 85.8, 85.0, 78.0, 76.9, 73.2, 72.5, 47.5, 42.3, 32.5, 31.6, 31.3, 24.4, 19.4, 18.3, 17.6, 17.5 ppm, IR (neat): 3309, 2956, 2912,

2870,1455, 1380, 1364, 1305, 1257, 1216, 1128, 1101, 1073, 1024, 977, 920, 877, 829, 795, 786, 752, 697 cm^{-1}. HRMS (ESI): m/z calcd for $C_{22}H_{32}O_3$ [M + Na]$^+$: 367.2249; found: 367.2263.

(1R,3aR,4S,5R,7R,8S,8aR)-8-(benzyloxy)-7-isopropyl-1,4-dimethyl-5-(vinyloxy)decahydro-4,7-epoxyazulene (3)

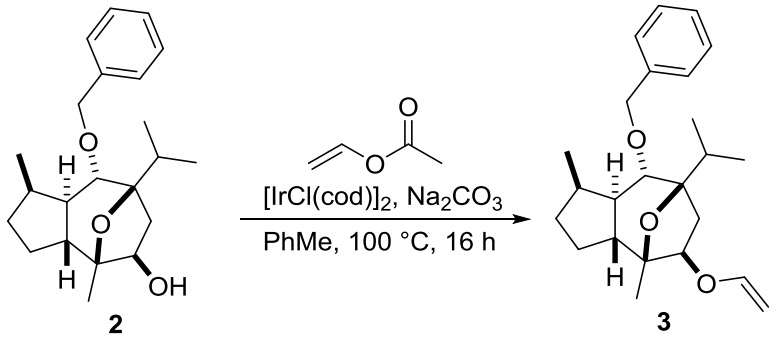

2 $C_{22}H_{32}O_3$ (344.50) **3** $C_{24}H_{34}O_3$ (370.53)

An oven-dried 10 mL Schlenk tube equipped with a Teflon-coated magnetic stirring bar was charged with $[IrCl(cod)]_2$ (3.90 mg, 5.81 μmol, 0.10 equiv) and Na_2CO_3 (36.9 mg, 348 μmol, 6.00 equiv) under an argon atmosphere. Dry PhMe (0.2 mL) was added followed by alcohol **2** (20.0 mg, 58.0 μmol, 1.00 equiv) in dry PhMe (0.2 mL) and dry vinyl acetate (107 μL, 1.16 mmol, 20.0 equiv). The reaction mixture was stirred for 16 h at 100 °C. The mixture was cooled down to 23 °C and was directly purified by flash chromatography on silica gel (pentane–Et_2O, 30:1) to give the ether **3** (17.7 mg, 47.8 μmol, 82%) as a clear oil.

$[\alpha]_D^{20}$ −82.8 (c 0.88, $CHCl_3$), ^{1}H NMR (700 MHz, $CDCl_3$) δ 7.38 – 7.27 (m, 4H), 7.32 – 7.23 (m, 1H), 6.35 (dd, J = 14.4, 6.8 Hz, 1H), 4.72 (d, J = 11.0 Hz, 1H), 4.60 (d, J = 11.0 Hz, 1H), 4.15 (dd, J = 14.4, 1.8 Hz, 1H), 4.02 (dd, J = 7.5, 2.8 Hz, 1H), 3.99 (dd, J = 6.8, 1.8 Hz, 1H), 3.52 (d, J = 9.7 Hz, 1H), 2.45 (dd, J = 14.3, 7.5 Hz, 1H), 2.46 – 2.40 (m, 1H), 2.09 (hept, J = 6.9 Hz, 1H), 1.97 (dddd, J = 13.8, 11.4, 8.0, 2.7 Hz, 1H), 1.74 (dd, J = 14.4, 2.7 Hz, 1H), 1.72 – 1.63 (m, 2H), 1.42 (ddd, J = 13.1, 9.7, 6.4 Hz, 1H), 1.32 – 1.26 (m, 1H), 1.25 (s, 3H), 1.14 – 1.06 (m, 1H), 1.04 (d, J = 7.0 Hz, 3H), 1.04 (d, J = 6.9 Hz, 3H), 0.98 (d, J = 7.1 Hz, 3H) ppm; ^{13}C NMR (176 MHz, $CDCl_3$) δ 150.6, 139.1, 128.5 (2C), 127.6, 127.3 (2C), 87.6, 86.1, 84.7, 78.6, 78.0, 72.6, 48.2, 47.9, 39.4, 32.6, 31.9, 31.4, 24.5, 19.5, 18.4, 17.7, 17.5 ppm; IR (neat): 2959, 2933, 2913, 2872, 1635, 1612, 1498, 1455, 1378, 1365, 1323, 1304, 1289, 1260, 1198, 1176, 1109, 1067, 1015, 998, 964, 947, 917, 890, 812, 736 cm^{-1}; HRMS (ESI): m/z calcd for $C_{24}H_{34}O_3$ [M + Na]$^+$: 393.2400; found: 393.2414.

2-(((1R,3aR,4S,5R,7R,8S,8aR)-8-(benzyloxy)-7-isopropyl-1,4-dimethyldecahydro-4,7-epoxyazulen-5-yl)oxy)ethan-1-ol (4)

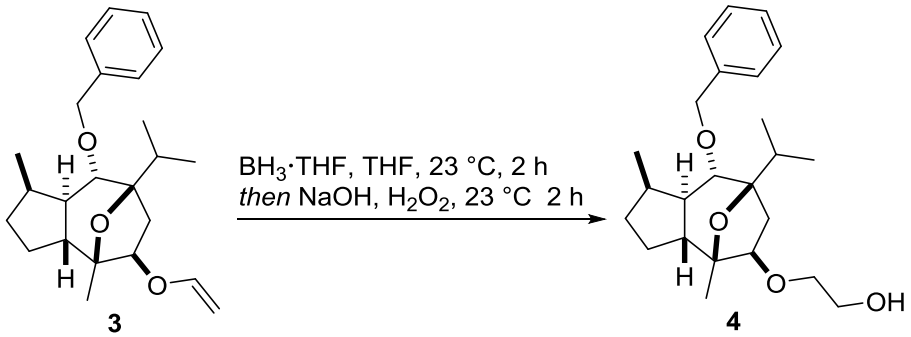

3 $C_{24}H_{34}O_3$ (370.53) **4** $C_{24}H_{36}O_4$ (388.55)

An oven-dried 5 mL round-bottom-flask equipped with a Teflon-coated magnetic stirring bar was charged with vinyl ether **3** (17.7 mg, 48.0 µmol, 1.00 equiv) and dry THF (1.4 mL) under an argon atmosphere. The solution was cooled to 0 °C and BH_3·THF (1M in THF) (0.30 mL, 300 µmol, 6.30 equiv) was slowly added at this temperature. The reaction was stirred for 2 h at 23 °C and then cooled down to 0 °C. NaOH (aq. 5 M, 0.70 mL) and H_2O_2 (30%, 1.40 mL) was added at 0 °C, the mixture was allowed to warm up to 23 °C and stirred for 2 h at 23 °C. The reaction mixture was diluted with dest. H_2O (1.0 mL) and extracted with Et_2O (4 × 2 mL). The combined organic phases were washed with sat. $Na_2S_2O_3$ solution and dried over sodium sulfate. The solvent was removed under reduced pressure and the crude product purified by flash chromatography on silica gel (pentane–Et_2O, 2:1) to give the alcohol **4** (15.0 mg, 38.6 µmol, 81%) as a clear oil.

$[\alpha]_D^{21}$ −51.4 (c 0.49, $CHCl_3$), ^{1}H NMR (700 MHz, $CDCl_3$) δ 7.37 – 7.26 (m, 4H), 7.31 – 7.22 (m, 1H), 4.70 (d, J = 11.0 Hz, 1H), 4.59 (d, J = 11.0 Hz, 1H), 3.77 – 3.65 (m, 2H), 3.59 (dd, J = 7.4, 2.8 Hz, 1H), 3.55 (ddd, J = 9.4, 5.7, 3.6 Hz, 1H), 3.50 (d, J = 9.7 Hz, 1H), 3.39 (ddd, J = 9.5, 5.6, 3.7 Hz, 1H), 2.45 – 2.36 (m, 1H), 2.37 (dd, J = 13.9, 7.4 Hz, 1H), 2.08 (hept, J = 6.9 Hz, 1H), 2.01 – 1.89 (m, 2H), 1.72 (dd, J = 13.9, 2.8 Hz, 1H), 1.73 – 1.58 (m, 2H), 1.36 (ddd, J = 13.0, 9.7, 6.3 Hz, 1H), 1.30 – 1.25 (m, 1H), 1.24 (s, 3H), 1.09 – 1.05 (m, 1H), 1.04 (d, J = 6.8 Hz, 3H), 1.04 (d, J = 7.0 Hz, 3H), 0.97 (d, J = 7.1 Hz, 3H) ppm; ^{13}C NMR (176 MHz, $CDCl_3$) δ 139.2, 128.4 (2C), 127.5, 127.3 (2C), 86.0, 85.0, 80.7, 78.0, 72.5, 70.1, 62.1, 48.2, 47.8, 39.2, 32.6, 32.4, 31.4, 24.5, 19.3, 18.5, 17.8, 17.5 ppm; IR (neat): 3447, 2957, 2932, 2873, 1455, 1379, 1304, 1260, 1212, 1156, 1109, 1066, 1022, 990, 925, 891, 749, 737 cm^{-1}; HRMS (ESI): m/z calcd for $C_{24}H_{36}O_4$ $[M + Na]^+$: 411.2506; found: 411.2518.

(2-(((1R,3aR,4S,5R,7R,8S,8aR)-8-(benzyloxy)-7-isopropyl-1,4-dimethyldecahydro-4,7-epoxyazulen-5-yl)oxy)ethoxy)(tert-butyl)dimethylsilane (5)

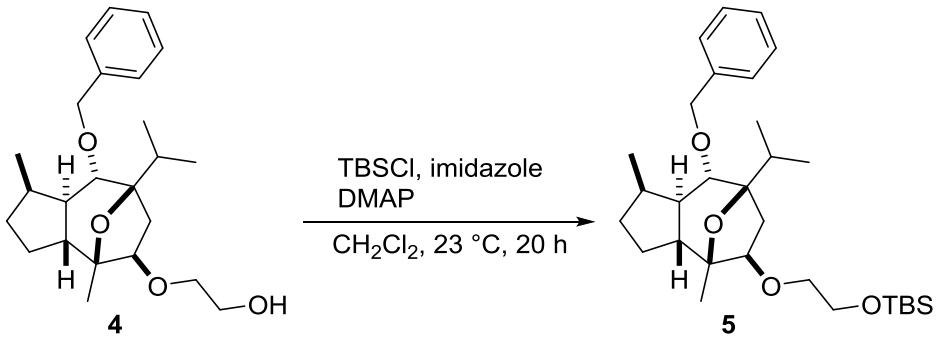

4 $C_{24}H_{36}O_4$ (388.55) **5** $C_{30}H_{50}O_4Si$ (502.81)

An oven-dried 5 mL round-bottom-flask equipped with a Teflon-coated magnetic stirring bar was charged with alcohol **4** (15.0 mg, 38.6 μmol, 1.00 equiv) and dry CH_2Cl_2 (0.60 mL) under an argon atmosphere. TBSCl (11.6 mg, 77.2 μmol, 2.00 equiv), imidazole (8.70 mg, 127 μmol, 3.30 equiv) and DMAP (0.70 mg, 6.00 μmol, 0.15 equiv) were added at 23 °C and the mixture was stirred for 20 h at this temperature. The reaction was quenched with sat. $NaHCO_3$ solution (5 mL) and extracted with CH_2Cl_2 (3 × 10 mL). The combined organic phases were dried over sodium sulfate and the solvent was removed under reduced pressure. The crude product was purified by flash chromatography on silica gel (pentane–Et_2O, 25:1) to give the silyl ether **5** (15.0 mg, 29.8 μmol, 77%) as a clear oil.

$[\alpha]_D^{20}$ −37.8 (c 1.00, $CHCl_3$), ^{1}H NMR (700 MHz, $CDCl_3$) δ 7.34 – 7.30 (m, 4H), 7.28 – 7.25 (m, 1H), 4.70 (d, J = 11.1 Hz, 1H), 4.59 (d, J = 11.1 Hz, 1H), 3.76 – 3.70 (m, 2H), 3.59 (dd, J = 7.5, 2.9 Hz, 1H), 3.51 – 3.46 (m, 2H), 3.40 – 3.35 (m, 1H), 2.42 – 2.37 (m, 1H), 2.35 (dd, J = 13.9, 7.5 Hz, 1H), 2.07 (hept, J = 6.8 Hz, 1H), 1.94 (dddd, J = 14.0, 11.4, 8.0, 2.6 Hz, 1H), 1.73 (dd, J = 13.8, 2.8 Hz, 1H), 1.69 – 1.59 (m, 2H), 1.36 (ddd, J = 13.0, 9.7, 6.3 Hz, 1H), 1.30 – 1.24 (m, 1H), 1.23 (s, 3H), 1.10 – 1.05 (m, 1H), 1.04 (t, J = 6.7 Hz, 6H), 0.96 (d, J = 7.1 Hz, 3H), 0.90 (s, 9H), 0.07 (s, 3H), 0.07 (s, 3H) ppm; ^{13}C NMR (176 MHz, $CDCl_3$) δ 139.3, 128.4 (2C), 127.5, 127.3 (2C), 85.9, 85.1, 80.7, 78.2, 72.5, 70.9, 63.0, 48.1, 47.9, 39.3, 32.6, 32.3, 31.4, 26.1 (3C), 24.4, 19.4, 18.5, 18.5, 17.9, 17.5, -5.1, -5.1 ppm; IR (neat): 2955, 2929, 2870, 1471, 1462, 1380, 1363, 1302, 1255, 1214, 1134, 1100, 1067, 1021, 991, 954, 835, 811, 777, 750, 735 cm^{-1}; HRMS (ESI): m/z calcd for $C_{30}H_{50}O_4Si$ $[M + Na]^+$: 525.3370; found: 525.3389.

(1R,3aR,4S,5R,7R,8S,8aR)-5-(2-((tert-butyldimethylsilyl)oxy)ethoxy)-7-isopropyl-1,4-dimethyldecahydro-4,7-epoxyazulen-8-ol (6)

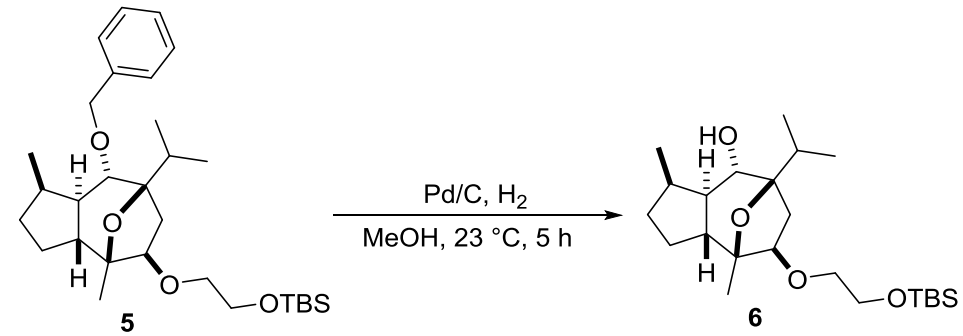

5 $C_{30}H_{50}O_4Si$ (502.81)

6 $C_{23}H_{44}O_4Si$ (412.69)

An oven-dried 5 mL round-bottom-flask equipped with a Teflon-coated magnetic stirring bar was charged with silyl ether **5** (15.0 mg, 29.8 μmol, 1.00 equiv) and MeOH (1.0 mL). Pd/C (dry, 20 wt%) (4.20 mg, 6.00 μmol, 0.20 equiv) was added and the reaction atmosphere was saturated with hydrogen by three times evacuating and setting under H_2 atmosphere. The reaction was stirred 5 h at 23 °C under an H_2 atmosphere (1 bar). The suspension was filtered over kieselgur and the product was eluted with MeOH (20 mL). The solvent was removed under reduced pressure and the crude product purified by flash chromatography on silica gel (pentane–Et_2O, 3:1) to give the alcohol **6** (9.00 mg, 21.8 mmol, 73%) as a clear oil.

$[\alpha]_D^{21}$ −62.5 (c 1.00, $CHCl_3$), ^{1}H NMR (700 MHz, $CDCl_3$) δ 3.78 – 3.72 (m, 2H), 3.64 (d, J = 10.2 Hz, 1H), 3.59 (dd, J = 7.4, 2.8 Hz, 1H), 3.53 – 3.49 (m, 1H), 3.41 (dt, J = 10.3, 5.3 Hz, 1H), 2.35 – 2.28 (m, 1H), 2.27 (dd, J = 13.8, 7.4 Hz, 1H), 2.02 – 1.96 (m, 2H), 1.71 (dd, J = 14.1, 2.6 Hz, 1H), 1.71 – 1.67 (m, 1H), 1.59 – 1.54 (m, 1H), 1.24 (s, 3H), 1.23 – 1.18 (m, 2H), 1.13 – 1.08 (m, 1H), 1.07 (d, J = 6.8 Hz, 3H), 1.07 (d, J = 7.1 Hz, 3H), 0.91 (s, 9H), 0.90 (d, J = 7.2 Hz, 3H), 0.09 (s, 3H), 0.09 (s, 3H) ppm; ^{13}C NMR (176 MHz, $CDCl_3$) δ 85.7, 85.3, 80.9, 71.2, 71.0, 63.0, 48.2, 48.0, 38.9, 32.7, 31.5, 30.7, 26.1 (3C), 25.9, 19.3, 18.6, 18.5, 17.7, 17.1, -5.1, -5.1 ppm; IR (neat): 3439, 2954, 2930, 2867, 1471, 1463, 1383, 1363, 1300, 1255, 1215, 1136, 1101, 1043, 1021, 1003, 953, 923, 903, 888, 835, 812, 777, 734 cm^{-1}; HRMS (ESI): m/z calcd for $C_{23}H_{44}O_4Si$ $[M + Na]^+$: 435.2901; found: 435.2910.

(1R,3aR,4S,5R,7R,8S,8aR)-5-(2-((tert-butyldimethylsilyl)oxy)ethoxy)-7-isopropyl-1,4-dimethyldecahydro-4,7-epoxyazulen-8-yl cinnamate (7)

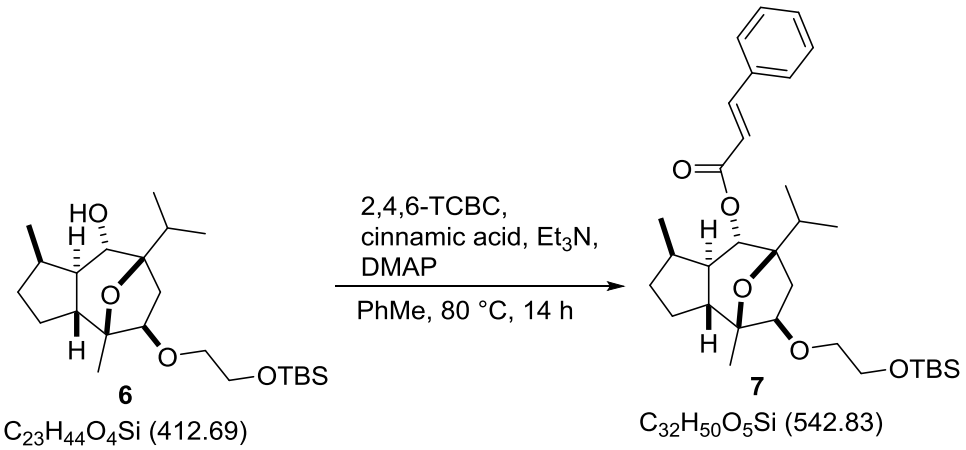

An oven-dried 5 mL round-bottom-flask equipped with a Teflon-coated magnetic stirring bar was charged with cinnamic acid (19.4 mg, 131 μmol, 4.00 equiv) and dry PhMe (0.27 mL) under an argon atmosphere. Et_3N (45.3 μL, 327 μmol, 10.0 equiv) and 2,4,6-trichlorbenzoylchloride (21.5 μL, 137 μmol, 4.20 equiv) were added at 23 °C. The reaction mixture was stirred for 1 h at 23 °C. DMAP (18.4 mg, 150 μmol, 4.60 equiv) and alcohol **6** (13.5 mg, 32.7 μmol, 1.00 equiv) were added to the reaction, the flask was sealed and stirred for 14 h at 80 °C. The reaction was quenched by adding sat. $NaHCO_3$ solution (3 mL) and the mixture was extracted with Et_2O (2 × 20 mL). The organic phase was dried over sodium sulfate and the solvent was removed under reduced pressure. The crude product was purified by flash chromatography on silica gel (pentane–Et_2O, 12:1) to give the ester **7** (13.9 mg, 25.6 μmol, 78%) as a clear oil.

$[\alpha]_D^{20}$ −58.9 (c 1.00, $CHCl_3$), ^1H NMR (700 MHz, $CDCl_3$) δ 7.66 (d, J = 16.0 Hz, 1H), 7.54 – 7.51 (m, 2H), 7.41 – 7.37 (m, 3H), 6.39 (d, J = 16.0 Hz, 1H), 5.10 (d, J = 10.3 Hz, 1H), 3.79 – 3.73 (m, 2H), 3.69 (dd, J = 7.5, 3.0 Hz, 1H), 3.55 – 3.51 (m, 1H), 3.48 – 3.38 (m, 1H), 2.46 (dd, J = 13.8, 7.4 Hz, 1H), 2.13 – 2.07 (m, 1H), 1.94 – 1.85 (m, 2H), 1.81 (dd, J = 13.7, 2.8 Hz, 1H), 1.76 – 1.68 (m, 2H), 1.44 (ddd, J = 13.2, 10.3, 6.5 Hz, 1H), 1.26 (s, 3H), 1.25 – 1.21 (m, 1H), 1.12 (dd, J = 11.3, 7.3 Hz, 1H), 1.02 (d, J = 6.8 Hz, 3H), 0.96 (d, J = 7.1 Hz, 3H), 0.94 (d, J = 7.1 Hz, 3H), 0.91 (s, 9H), 0.09 (s, 3H), 0.08 (s, 3H) ppm; ^{13}C NMR (176 MHz, $CDCl_3$) δ 165.8, 145.0, 134.5, 130.5, 129.0 (2C), 128.2 (2C), 118.4, 85.4, 85.3, 80.8, 71.9, 71.1, 63.0, 47.8, 47.0, 40.2, 33.5, 31.3, 31.2, 26.1 (3C), 25.0, 19.3, 18.5 (2C), 17.8, 17.1, -5.1, -5.1 ppm; IR (neat): 2954, 2930, 2882, 2857, 1713, 1637, 1471, 1463, 1450, 1384, 1368, 1333, 1302, 1280, 1254, 1202, 1170, 1138, 1100, 1042, 1014, 979, 955, 926, 835, 812, 777, 767, 709 cm^{-1}; HRMS (ESI): m/z calcd for $C_{32}H_{50}O_5Si$ $[M + Na]^+$: 565.3320; found: 565.3339.

(1R,3aR,4S,5R,7R,8S,8aR)-5-(2-hydroxyethoxy)-7-isopropyl-1,4-dimethyldecahydro-4,7-epoxyazulen-8-yl cinnamate (1)

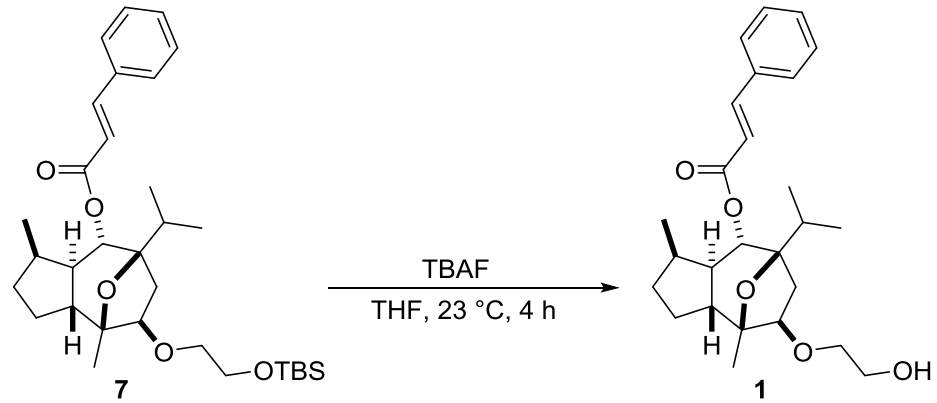

7 $C_{32}H_{50}O_5Si$ (542.83) **1** $C_{26}H_{36}O_5$ (428.57)

An oven-dried 5 mL round-bottom-flask equipped with a Teflon-coated magnetic stirring bar was charged with ester **7** (13.6 mg, 25.1 μmol, 1.00 equiv) and dry THF (0.10 mL) under an argon atmosphere. TBAF solution (1M in THF) (62.6 μL, 62.6 μmol, 2.50 equiv) was added at 0 °C. The reaction was allowed to warm up to 23 °C and stirred for 4 h at this temperature. After this time dest. H_2O was added to quench the reaction. The aqueous phase was extracted with Et_2O (3 × 20 mL). The combined organic phases were dried over sodium sulfate and the solvent was removed under reduced pressure. The crude product was purified by flash chromatography on silica gel (pentane–Et_2O, 1:1) to give the alcohol **1** (10.6 mg, 24.7 μmol, 99%) as a clear oil.

$[\alpha]_D^{20}$ −63.8 (c 1.00, $CHCl_3$), ^{1}H NMR (700 MHz, $CDCl_3$) δ 7.66 (d, J = 16.0 Hz, 1H), 7.52 (ddd, J = 5.9, 2.9, 1.9 Hz, 2H), 7.42 – 7.35 (m, 3H), 6.39 (d, J = 16.0 Hz, 1H), 5.12 (d, J = 10.3 Hz, 1H), 3.80 – 3.68 (m, 2H), 3.68 (dd, J = 7.4, 2.9 Hz, 1H), 3.60 (ddd, J = 9.4, 5.8, 3.5 Hz, 1H), 3.45 (ddd, J = 9.4, 5.6, 3.6 Hz, 1H), 2.49 (dd, J = 13.8, 7.4 Hz, 1H), 2.17 – 2.05 (m, 1H), 1.97 – 1.84 (m, 2H), 1.79 (dd, J = 13.9, 2.7 Hz, 1H), 1.77 – 1.70 (m, 2H), 1.44 (ddd, J = 13.2, 10.3, 6.5 Hz, 1H), 1.27 (s, 3H), 1.26 – 1.22 (m, 1H), 1.11 (dd, J = 11.3, 7.3 Hz, 1H), 1.02 (d, J = 6.8 Hz, 3H), 0.96 (d, J = 7.1 Hz, 3H), 0.94 (d, J = 7.1 Hz, 3H) ppm; ^{13}C NMR (176 MHz, $CDCl_3$) δ 165.8, 145.1, 134.5, 130.5, 129.0 (2C), 128.2 (2C), 118.3, 85.4, 85.4, 80.7, 71.7, 70.4, 62.1, 47.7, 47.0, 40.2, 33.6, 31.3, 31.2, 25.0, 19.2, 18.5, 17.7, 17.1 ppm; IR (neat): 3453, 2956, 2933, 2872, 1710, 1636, 1496, 1449, 1368, 1334, 1303, 1268, 1202, 1170, 1138, 1107, 1072, 1043, 1014, 981, 956, 926, 891, 815, 798, 767, 738, 723, 710, 686, 659 cm^{-1}; HRMS (ESI): m/z calcd for $C_{26}H_{36}O_5$ $[M + H]^+$: 429.2636; found: 429.2635.

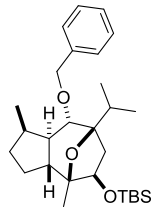
O
H
O
H
OTBS

B

4.09
1.76
1.01
1.02
1.01
1.01
2.10
1.04
1.03
3.09
0.99
1.09
3.00
5.90
0.98
3.02
8.96
3.07
2.96
12.0 11.5 11.0 10.5 10.0 9.5 9.0 8.5 8.0 7.5 7.0 6.5 6.0 5.5 5.0 4.5 4.0 3.5 3.0 2.5 2.0 1.5 1.0 0.5 0.0 -0.5
Chemical Shift (ppm)

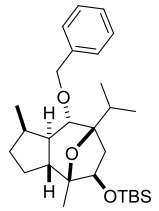
O
H
O
H
OTBS

B

139.3
128.4
127.5
127.4
85.8
85.4
78.2
73.0
72.6
48.1
47.6
42.8
32.6
32.0
31.4
25.9
24.6
19.9
18.5
18.3
17.7
17.6
-4.5
-4.9
220 210 200 190 180 170 160 150 140 130 120 110 100 90 80 70 60 50 40 30 20 10 0 -10
Chemical Shift (ppm)

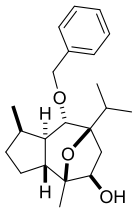
O
H
O
H
OH

2

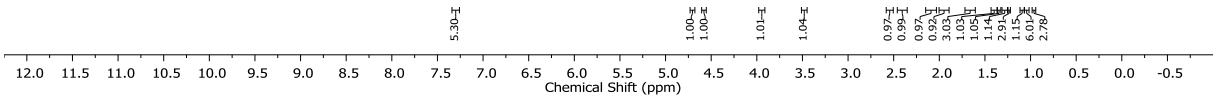
5.30
1.00
1.00
1.01
1.04
0.97
0.99
0.97
0.92
3.03
1.03
1.05
1.14
2.91
1.15
6.01
2.78

12.0 11.5 11.0 10.5 10.0 9.5 9.0 8.5 8.0 7.5 7.0 6.5 6.0 5.5 5.0 4.5 4.0 3.5 3.0 2.5 2.0 1.5 1.0 0.5 0.0 -0.5
Chemical Shift (ppm)

139.2
128.4
127.6
127.3
85.8
85.1
78.0
73.3
72.6
47.9
47.5
42.3
32.6
31.7
31.4
24.4
19.5
18.3
17.7
17.5

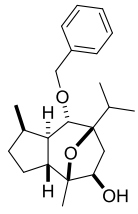
O
H
O
H
OH

2

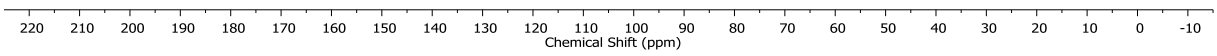
220 210 200 190 180 170 160 150 140 130 120 110 100 90 80 70 60 50 40 30 20 10 0 -10
Chemical Shift (ppm)

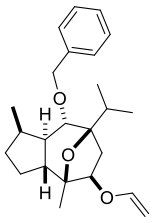

3

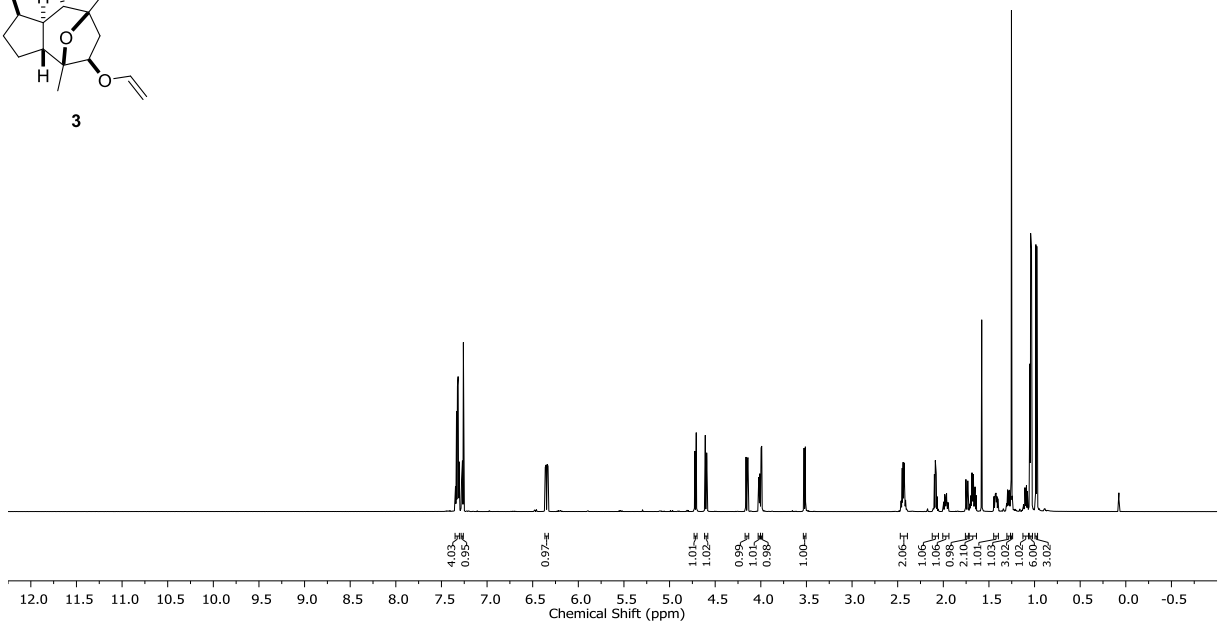
4.03
0.95
0.97
1.01
1.02
0.99
1.01
0.98
1.00
2.06
1.05
1.06
0.98
2.10
1.01
1.03
3.02
1.02
6.00
3.02
12.0 11.5 11.0 10.5 10.0 9.5 9.0 8.5 8.0 7.5 7.0 6.5 6.0 5.5 5.0 4.5 4.0 3.5 3.0 2.5 2.0 1.5 1.0 0.5 0.0 -0.5
Chemical Shift (ppm)

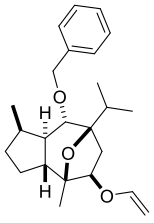

3

150.6
139.1
128.5
127.6
127.3
87.6
86.1
84.7
78.6
78.0
72.6
48.2
47.9
39.4
32.6
31.9
31.4
24.5
19.5
18.4
17.7
17.5
220 210 200 190 180 170 160 150 140 130 120 110 100 90 80 70 60 50 40 30 20 10 0 -10
Chemical Shift (ppm)

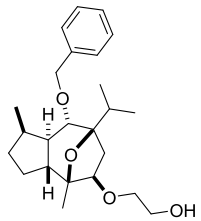
O
H
O
H
O
OH

4

4.01
0.99
0.99
1.00
1.98
0.98
0.98
0.99
0.98
1.08
0.97
0.98
1.71
0.94
1.94
0.99
1.09
3.00
0.80
6.08
3.00
12.0 11.5 11.0 10.5 10.0 9.5 9.0 8.5 8.0 7.5 7.0 6.5 6.0 5.5 5.0 4.5 4.0 3.5 3.0 2.5 2.0 1.5 1.0 0.5 0.0 -0.5
Chemical Shift (ppm)

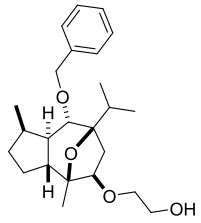
O
H
O
H
O
OH

4

139.2
128.4
127.5
127.3
86.0
85.0
80.7
78.0
72.5
70.1
62.1
48.2
47.8
39.2
32.6
32.4
31.4
24.5
19.3
18.5
17.8
17.5
220 210 200 190 180 170 160 150 140 130 120 110 100 90 80 70 60 50 40 30 20 10 0 -10
Chemical Shift (ppm)

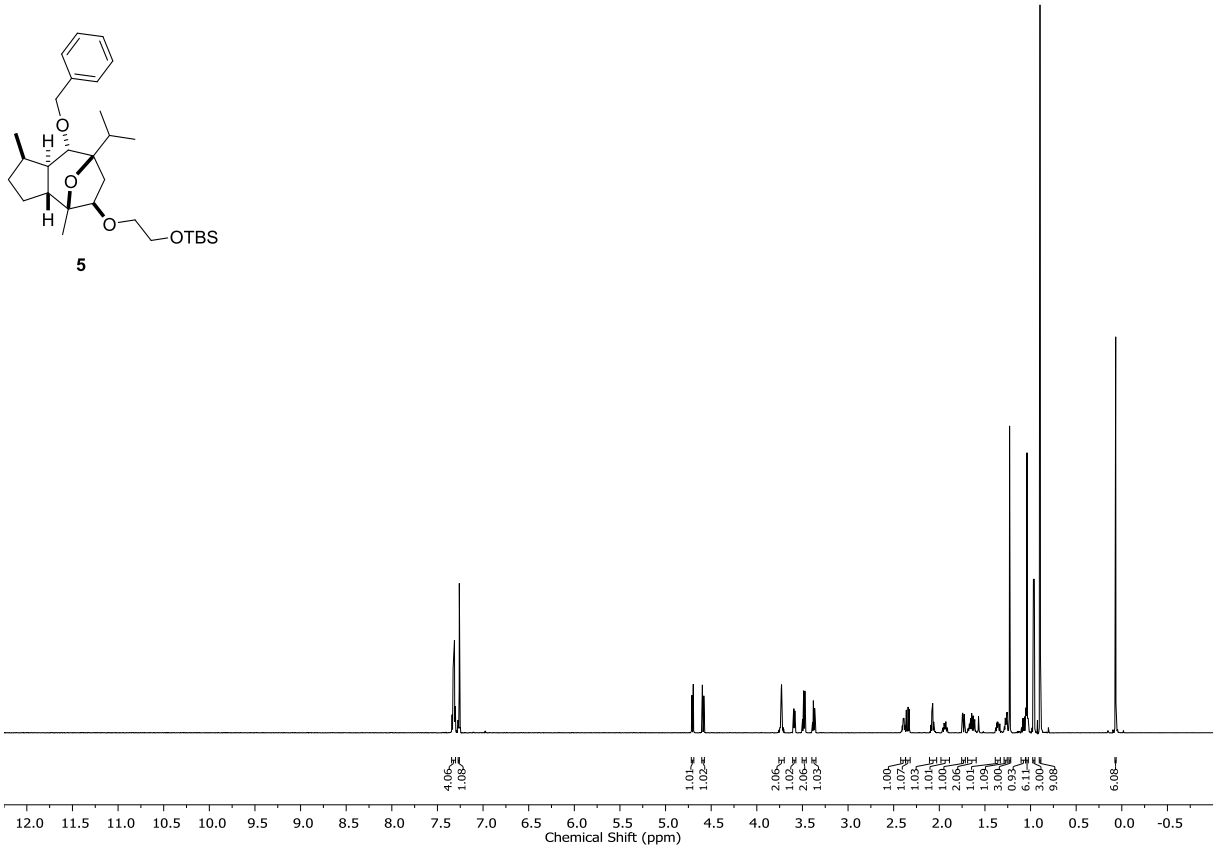
OTBS
5
4.06
1.08
1.01
1.02
2.06
1.02
2.06
1.03
1.00
1.07
1.03
1.01
1.00
2.06
1.01
1.09
3.00
0.93
6.11
3.00
9.08
6.08
12.0 11.5 11.0 10.5 10.0 9.5 9.0 8.5 8.0 7.5 7.0 6.5 6.0 5.5 5.0 4.5 4.0 3.5 3.0 2.5 2.0 1.5 1.0 0.5 0.0 -0.5
Chemical Shift (ppm)

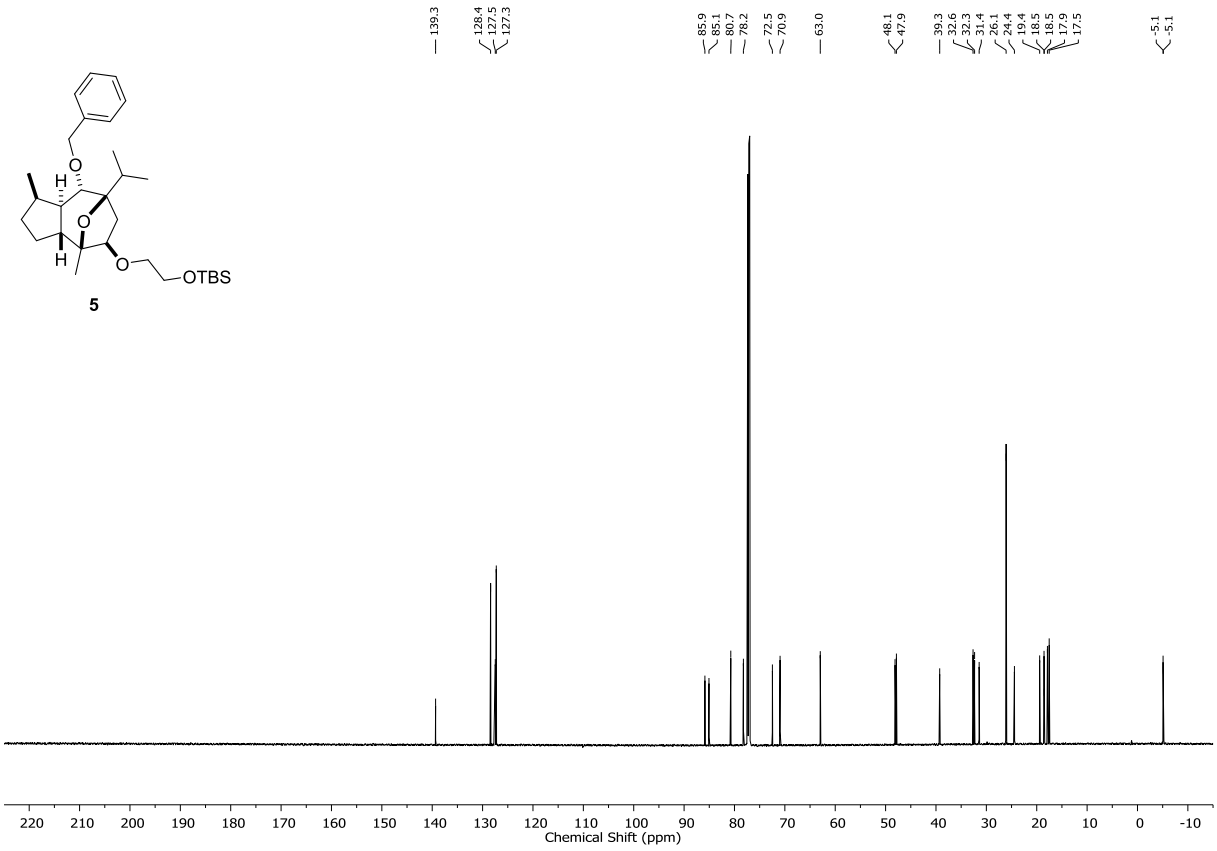
139.3
128.4
127.5
127.3
85.9
85.1
80.7
78.2
72.5
70.9
63.0
48.1
47.9
39.3
32.6
32.3
31.4
26.1
24.4
19.4
18.5
18.5
17.9
17.5
-5.1
-5.1
OTBS
5
220 210 200 190 180 170 160 150 140 130 120 110 100 90 80 70 60 50 40 30 20 10 0 -10
Chemical Shift (ppm)

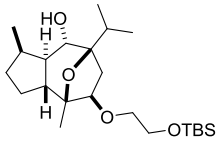
HO
H
O
H
O
OTBS

6

2.01
0.98
0.99
1.00
1.00
0.99
1.00
2.01
1.97
0.99
3.08
2.01
0.81
6.06
8.78
3.07
6.01
12.0 11.5 11.0 10.5 10.0 9.5 9.0 8.5 8.0 7.5 7.0 6.5 6.0 5.5 5.0 4.5 4.0 3.5 3.0 2.5 2.0 1.5 1.0 0.5 0.0 -0.5
Chemical Shift (ppm)

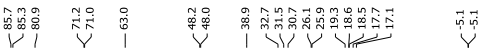
85.7
85.3
80.9
71.2
71.0
63.0
48.2
48.0
38.9
32.7
31.5
30.7
26.1
25.9
19.3
18.6
18.5
17.7
17.1
-5.1
-5.1

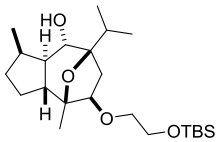
HO
H
O
H
O
OTBS

6

220 210 200 190 180 170 160 150 140 130 120 110 100 90 80 70 60 50 40 30 20 10 0 -10
Chemical Shift (ppm)

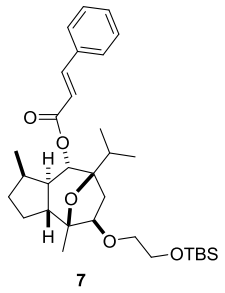
O
O
H
O
H
O
OTBS

7

1.00
2.03
3.05
1.00
1.00
2.02
1.01
1.00
1.00
0.99
1.00
2.00
1.00
1.98
0.97
3.10
1.10
0.85
2.97
5.94
9.09
6.02
12.0 11.5 11.0 10.5 10.0 9.5 9.0 8.5 8.0 7.5 7.0 6.5 6.0 5.5 5.0 4.5 4.0 3.5 3.0 2.5 2.0 1.5 1.0 0.5 0.0 -0.5
Chemical Shift (ppm)

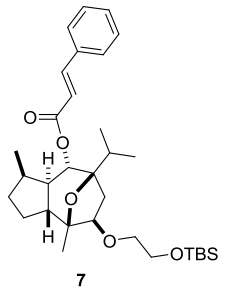
O
O
H
O
H
O
OTBS

7

165.8
145.0
134.5
130.5
129.0
128.2
118.4
85.4
85.3
80.8
71.9
71.1
63.0
47.8
47.0
40.2
33.5
31.3
31.2
26.1
25.0
19.3
18.5
17.8
17.1
-5.1
-5.1
220 210 200 190 180 170 160 150 140 130 120 110 100 90 80 70 60 50 40 30 20 10 0 -10
Chemical Shift (ppm)

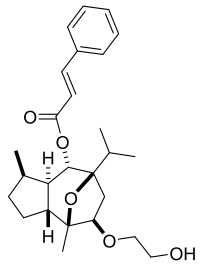
O
O
H
O
H
O
OH

1

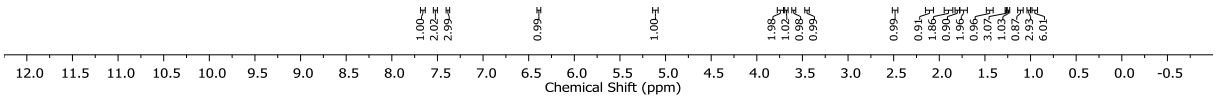
1.00
2.02
2.99
0.99
1.00
1.98
1.02
0.98
0.99
0.99
0.91
1.86
0.90
1.96
0.96
3.07
1.03
0.87
2.93
6.01

12.0 11.5 11.0 10.5 10.0 9.5 9.0 8.5 8.0 7.5 7.0 6.5 6.0 5.5 5.0 4.5 4.0 3.5 3.0 2.5 2.0 1.5 1.0 0.5 0.0 -0.5
Chemical Shift (ppm)

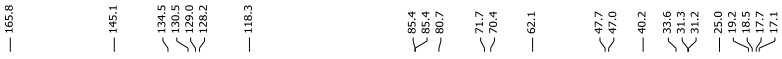
165.8
145.1
134.5
130.5
129.0
128.2
118.3
85.4
85.4
80.7
71.7
70.4
62.1
47.7
47.0
40.2
33.6
31.3
31.2
25.0
19.2
18.5
17.7
17.1

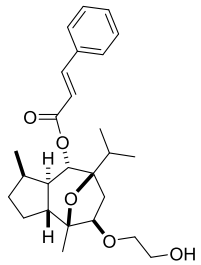
O
O
H
O
H
O
OH

1

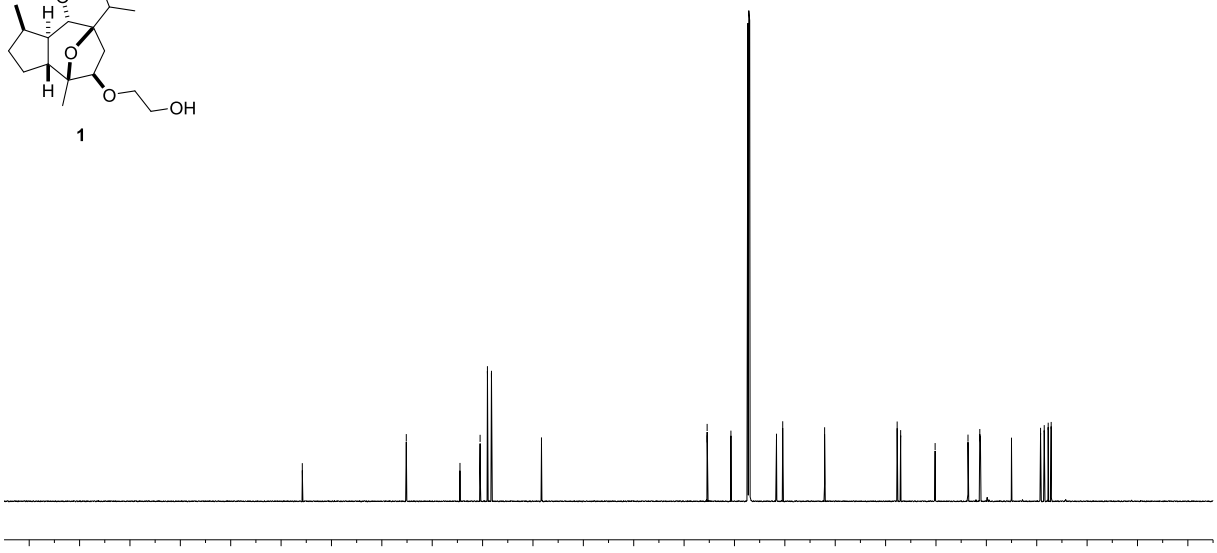
220 210 200 190 180 170 160 150 140 130 120 110 100 90 80 70 60 50 40 30 20 10 0 -10
Chemical Shift (ppm)